International Journal of Solids and Structures 50 (2013) 160–175

Contents lists available at SciVerse ScienceDirect

International Journal of Solids and Structures

journal homepage: www.elsevier.com/locate/ijsolstr

Line-integral representations of the displacement and stress fields due to an arbitrary Volterra dislocation loop in a transversely isotropic elastic full space

J.H. Yuan [a], W.Q. Chen [b], E. Pan [c,d,*]

[a] Department of Civil Engineering, Zhejiang University, Hangzhou 310058, China
[b] Department of Engineering Mechanics, Zhejiang University, Hangzhou 310027, China
[c] Department of Civil Engineering and Department of Applied Mathematics, University of Akron, Akron, OH 44325, USA
[d] School of Mechanical Engineering, Zhengzhou University, Zhengzhou 450001, China

ARTICLE INFO

Article history:
Received 21 June 2012
Received in revised form 4 September 2012
Available online 18 September 2012

Keywords:
Line integral representation
Dislocation loop
Dislocation segment
Solid angle
Transverse isotropy
Hexagonal crystals
Elastic field

ABSTRACT

Transversely isotropic materials or hexagonal crystals are commonly utilized in various engineering fields; however, dislocation solutions for such special materials have not been fully developed. In this paper, we present a comprehensive study on this important topic, where only Volterra dislocations of the translational type are considered. Based on the potential theory of linear elasticity, we extend the well-known Burgers displacement equation for an arbitrarily shaped dislocation loop in an isotropic elastic full space to the transversely isotropic case. Both the induced displacements and stresses are expressed uniformly in terms of simple and explicit line integrals along the dislocation loop. We introduce three quasi solid angles to describe the displacement discontinuities over the dislocation surface and extract a simple step function out of these angles to characterize the dependence of the displacements on the configuration of the dislocation surface. We also give a new explicit formula for calculating accurately and efficiently the traditional solid angle of an arbitrary polygonal dislocation loop. From the present line-integral representations, exact closed-form solutions in terms of elementary functions are further obtained in a unified way for the displacement and stress fields due to a straight dislocation segment of arbitrary orientation. The non-uniqueness of the elastic field solution due to an open dislocation segment is rigorously discussed and demonstrated. For a circular dislocation loop parallel to the plane of isotropy, a new explicit expression of the induced elastic field is presented in terms of complete elliptic integrals. Several numerical examples are also provided as illustration and verification of the derived dislocation solutions, which further show the importance of material anisotropy on the dislocation-induced elastic field, and reveal the non-uniqueness feature of the elastic field due to a straight dislocation segment.

1. Introduction

On the mesoscopic scale, dislocations play a crucial role in understanding the plasticity and strength of crystalline materials. As a powerful tool in mesoscale simulation, three-dimensional (3D) dislocation dynamics (DD) predicts macroscopic properties of crystals by directly simulating the interaction and evolution of large groups of discrete and randomly distributed dislocation lines within crystals in response to external loads (Kubin et al., 1992; Devincre and Condat, 1992; Zbib et al., 1998, 2000; Rhee et al., 1998; Verdier et al., 1998; Schwarz, 1999; Ghoniem and Sun, 1999; Ghoniem et al., 2000; Cai et al., 2004; Wang et al., 2006; Arsenlis et al., 2007). For instance, DD simulations have been successfully utilized to study the effect of cross-slip and short-range interactions on dislocation patterning (Devincre and Kubin, 1997; Devincre et al., 2001; Madec et al., 2002), the role of collinear dislocation interaction in multislip hardening of fcc metals (Madec et al., 2003), the plastic anisotropy of flow stress in fcc single crystals (Wang et al., 2009), the size-dependence of flow stress in fcc metallic micro-pillars under uniaxial loading in the absence of strain gradients (Senger et al., 2008; Weygand et al., 2008), the difference in dislocation behavior and strengthening mechanism between fcc and bcc sub-micrometer pillars under uniaxial compression (Greer et al., 2008), the size-dependent plasticity in polycrystalline thin films (von Blanckenhagen et al., 2004; Espinosa et al., 2006; Zhou and LeSar, 2012).

In 3D-DD simulations, dislocation lines are discretized into a set of straight or curved dislocation segments of arbitrary orientations with general Burgers vectors. The computation of long-range pair interactions among these dislocation segments is very time-consuming, mostly on the evaluation of the stress field of one segment on another segment. For the sake of computational simplicity

* Corresponding author at: Department of Civil Engineering and Department of Applied Mathematics, University of Akron, Akron, OH 44325, USA. Tel.: +1 330 972 6739; fax: +1 330 972 6020.
E-mail addresses: yuanfyrc2005@yahoo.com.cn (J.H. Yuan), chenwq@zju.edu.cn (W.Q. Chen), pan2@uakron.edu (E. Pan).

0020-7683/$ - see front matter © 2012 Elsevier Ltd. All rights reserved.
http://dx.doi.org/10.1016/j.ijsolstr.2012.09.011

and time efficiency, nearly all DD simulations assume linear-elastic isotropy in spite of the fact that most of the crystalline materials exhibit anisotropy. Attempts were made to release this constraint by assuming general anisotropy in DD simulations (Rhee et al., 2001; Han et al., 2003). Particularly, Capolungo et al. (2010) introduced transverse isotropy in their DD simulations and found a substantial effect of the elastic anisotropy on strain hardening of hcp metals. In their work, they used Mura's formula (Hirth and Lothe, 1982) in anisotropic elasticity to calculate the stress field of dislocation segments in hcp metals. However, for the special case of hexagonal crystals, a numerically efficient stress formula in terms of simple line integrals can be developed.

Line-integral representations of the elastic field in crystals due to an arbitrarily shaped Volterra dislocation loop have attracted a great deal of attention due to their direct applications in 3D-DD simulations. For an arbitrary dislocation loop located in an isotropic elastic full space, the Burgers displacement equation (Burgers, 1939) and Peach–Koehler stress formulae (Peach and Koehler, 1950; deWit, 1960; Devincre, 1995) are the well-known line-integral solutions for the induced displacement and stress fields, respectively. For a generally anisotropic material which occupies the full space, once the associated Green's tensor is known, the Mura's formula enables us to express the gradient of displacements due to an arbitrary dislocation loop in terms of line integrals over the dislocation loop (Mura, 1963). Indenbom and Orlov (1967) generalized the work of Lothe (1967) and Brown (1967) by expressing the elastic distortions of a general dislocation loop in an anisotropic full space in terms of straight dislocations; they also converted the corresponding displacement field of such a dislocation loop to an elegant line-integral along the dislocation loop, with the integrand itself being also a single integral (Indenbom and Orlov, 1968). Willis (1970) expressed the distortions due to an infinite (or a finite) straight dislocation line in an anisotropic full space analytically in terms of the roots of a sextic equation; similarly Wang (1996) discussed the corresponding curved dislocation problem. Chu et al. (2011) derived a single-integral expression for the displacement field due to a dislocation loop of triangular shape in infinite anisotropic crystals. For a dislocation loop located in the basal plane of a hexagonal crystal, both the induced displacements and stresses can be transformed into explicit line integrals (Chou and Yang, 1973; Tupholme, 1974). In addition, Yu and Sanday (1994) derived analytical displacement solutions due to an infinitesimal dislocation loop of arbitrary orientation in a transversely isotropic full space. Ohr (1972, 1973) also obtained the elastic field solutions due to a prismatic or glide circular dislocation loop within the basal plane of an infinite hexagonal crystal.

Among various anisotropic materials, the transversely isotropic material is the only one whose Green's tensor takes a simple and explicit form. However, for an arbitrary Volterra dislocation loop in a transversely isotropic full space, an explicit line-integral formula for the induced displacement field, which resembles the Burgers displacement equation in the isotropic case, is still unavailable in the literature. In this paper, we attempt to fill this gap via the potential theory of linear elasticity and solve the displacement and stress fields in a transversely isotropic full space produced by (i) a Volterra dislocation loop of arbitrary shape and orientation; (ii) a straight dislocation segment of arbitrary orientation; (iii) a circular dislocation loop parallel to the plane of isotropy.

The present paper is organized as follows. In Section 2, for a simple Volterra dislocation loop which is mathematically defined in Eq. (7), we derive a line-integral representation of the induced displacement field in terms of three potential functions. As verification, in Section 3, our displacement solution is successfully reduced to the well-known Burgers displacement expression in the isotropic case. In Section 4, the line-integral expressions of the stresses due to a simple dislocation loop are then deduced from the displacement solution by virtue of the stress-displacement relations. In Section 5, the derived displacement and stress solutions are further simplified and expressed uniformly in terms of simple line integrals over the closed dislocation curve. Furthermore, the simplified elastic field solutions are reformulated via the principle of superposition so that they are applicable also to the case of complex dislocation loops. In Section 6, the general line-integral solutions for an arbitrary dislocation loop are utilized to develop exact closed-form solutions for a straight dislocation segment of arbitrary orientation. Moreover, the non-uniqueness feature of the dislocation segment solution is well demonstrated. A new explicit formula is also presented for calculating accurately and efficiently the traditional solid angle of an arbitrary polygonal dislocation loop. In Section 7, based on the general solutions, we deal with a circular dislocation loop parallel to the plane of isotropy and obtain a new explicit expression of the induced elastic field in terms of complete elliptic integrals. In Section 8, several numerical examples are provided to validate the present dislocation solutions, and to illustrate the non-uniqueness feature of the displacement and stress fields induced by a straight dislocation segment. Concluding remarks are drawn in Section 9.

2. Displacement field due to a simple dislocation loop

In the Cartesian coordinate system (x_1, x_2, x_3) (see Fig. 1), according to the theory of dislocations, the elastic displacement field induced by a Volterra dislocation loop C of arbitrary shape and orientation, which bounds some curved surface A, can be expressed as (Hirth and Lothe, 1982)

$$u_m(\mathbf{x}) = -\int_A \mathrm{d}A_i b_j c_{ijkl} \frac{\partial}{\partial y_l} u_{km}(\mathbf{y};\mathbf{x}) \tag{1}$$

where $u_m(\mathbf{x})$ is the mth component of the displacement vector at $\mathbf{x}$ (x_1, x_2, x_3), and $u_{km}(\mathbf{y};\mathbf{x})$ is the Green's tensor, denoting the kth component of the displacement vector at $\mathbf{y}$ (y_1, y_2, y_3) due to a unit force in the mth direction applied at $\mathbf{x}$ (x_1, x_2, x_3). c_{ijkl} is the elastic stiffness tensor, b_j is the jth component of the Burgers vector $\mathbf{b}$, and $\mathrm{d}A_i$ at $\mathbf{y}$ (y_1, y_2, y_3) is the ith component of the vector area element $\mathrm{d}\mathbf{A}$. The positive normal of $\mathrm{d}\mathbf{A}$ is associated with the positive direction of the dislocation curve according to the right-hand rule (Fig. 1).

Note that, in this paper, summation over a repeated (or multi-repeated) index is assumed unless this index occurs on both sides of an equation (or a relation). Also, the range of the Roman indices i, j, k etc. is from 1 to 3, and that of the Greek ones α, β, κ etc. is from 1 to 2, unless otherwise specified.

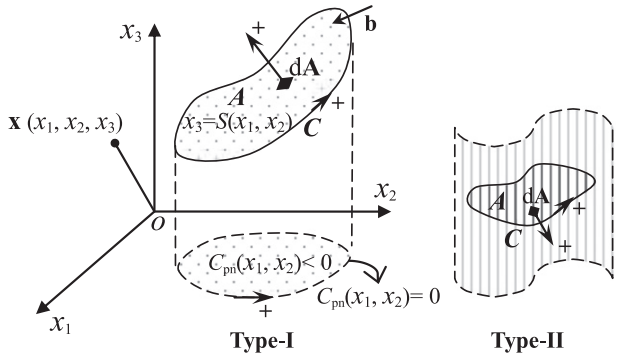

Fig. 1. Illustration of two types of simple dislocation loops in Cartesian coordinate system: Type-I shows a generally oriented loop, and Type-II shows a specially oriented loop which lies on a cylindrical surface with its generatrix parallel to the x_3-axis.

For a transversely isotropic material, if the plane of isotropy is assumed to be parallel to the x_1–x_2 plane, then the elastic stiffness tensor c_{ijkl} can be expressed as (Pan and Chou, 1976)

$$c_{ijkl} = a_1\delta_{ij}\delta_{kl} + a_2(\delta_{ik}\delta_{jl} + \delta_{il}\delta_{jk}) + a_3\delta_{i3}\delta_{j3}\delta_{k3}\delta_{l3} + a_4(\delta_{i3}\delta_{j3}\delta_{kl} + \delta_{k3}\delta_{l3}\delta_{ij}) + a_5(\delta_{j3}\delta_{k3}\delta_{il} + \delta_{i3}\delta_{l3}\delta_{jk} + \delta_{j3}\delta_{l3}\delta_{ik} + \delta_{i3}\delta_{k3}\delta_{jl}) \quad (2)$$

where δ_{ij} is the Kronecker delta, and a_n ($n = 1,2,\ldots,5$) are related to the contracted elastic stiffness constants c_{pq} ($p, q = 1,2,\ldots,6$) as

$$a_1 = c_{11} - 2c_{66}; \quad a_2 = c_{66}$$
$$a_3 = c_{11} + c_{33} - 2c_{13} - 4c_{44} \quad (3)$$
$$a_4 = c_{13} - c_{11} + 2c_{66}; \quad a_5 = c_{44} - c_{66}$$

Based on the potential theory of linear elasticity, the Green's tensor $u_{ij}(\mathbf{y};\mathbf{x})$ for a transversely isotropic full space can be expressed compactly in terms of the potential functions $\chi_i(\mathbf{y};\mathbf{x})$ as (Fabrikant, 2004)

$$u_{\alpha\beta} = u_{\beta\alpha} = \frac{1}{4\pi c_{44}}\left[\frac{\partial^2}{\partial y_\alpha \partial y_\beta}\left(\frac{m_2\gamma_1\chi_1 - m_1\gamma_2\chi_2}{m_1 - m_2} + \gamma_3\chi_3\right) + \delta_{\alpha\beta}\frac{\partial^2(\gamma_3^2\chi_3)}{\partial y_3^2}\right]$$
$$u_{\alpha 3} = u_{3\alpha} = \frac{1}{4\pi c_{44}}\frac{\partial^2}{\partial y_\alpha \partial y_3}\left(\frac{\gamma_1\chi_1 - \gamma_2\chi_2}{m_1 - m_2}\right) \quad (4)$$
$$u_{33} = \frac{1}{4\pi c_{44}}\frac{\partial^2}{\partial y_3^2}\left(\frac{m_1\gamma_1\chi_1 - m_2\gamma_2\chi_2}{m_1 - m_2}\right) \quad \text{for } m_1 \neq m_2$$

where the constants γ_i are defined as

$$\gamma_\alpha = \sqrt{\frac{c_{44} + m_\alpha(c_{13} + c_{44})}{c_{11}}} = \sqrt{\frac{m_\alpha c_{33}}{m_\alpha c_{44} + (c_{13} + c_{44})}};$$
$$\gamma_3 = \sqrt{c_{44}/c_{66}} \quad (5)$$

and m_α can be solved from Eq. (5) as

$$m_{1,2} = -1 + \frac{1}{2c_{44}(c_{13} + c_{44})} \times \left\{(c_{11}c_{33} - c_{13}^2) \pm \sqrt{(c_{11}c_{33} - c_{13}^2)[c_{11}c_{33} - (c_{13} + 2c_{44})^2]}\right\} \quad (6)$$

with $m_1 m_2 = 1$, and $c_{11}c_{33} - {c_{13}}^2 > 0$ from the elastic-energy consideration.

The potential function χ_i in Eq. (4) deserves further discussion for the specific problem of dislocation loops. In general, a complex dislocation loop could always be divided into a finite number of simple dislocation loops by adding certain auxiliary dislocation line pairs properly (see Fig. 2 for example). Without loss of generality, the solutions derived in this section and subsequent Sections 3 and 4 will be based upon the following simple loop assumptions (as shown in Fig. 1 for Type-I and Type-II):

(I) The dislocation surface bounded by the loop is simply connected and intersects at most once with an arbitrary straight line parallel to the x_3-axis, so it can always be described by a single-valued function

$$x_3 = S(x_1, x_2) \ \text{ with } \ C_{\text{pn}}(x_1, x_2) \leqslant 0 \quad (7)$$

where $C_{\text{pn}}(x_1, x_2) = 0$ with $x_3 = 0$ is the projection of this loop onto the x_1–x_2 plane, and the subscript "pn" just indicates projection.

(II) The dislocation surface bounded by the loop is simply connected and just lies on a cylindrical surface with its generatrix parallel to the x_3-axis. As such, its projection onto the x_1–x_2 plane degenerates into a line segment.

It is noted that Type-II can be considered as a limiting case of Type-I. Thus, our derivation below will mainly focus on the Type-I dislocation loop with additional discussion on Type-II when necessary. For a Type-I dislocation loop, the potential function χ_i can be properly selected as

$$\chi_i(\mathbf{y};\mathbf{x}) = \begin{cases} -\frac{y_3 - x_3}{\gamma_i}\ln\left(R_i - \frac{y_3 - x_3}{\gamma_i}\right) - R_i \\ \text{for } x_3 > S(x_1, x_2) \text{ with } C_{\text{pn}}(x_1, x_2) \leqslant 0 \\ +\frac{y_3 - x_3}{\gamma_i}\ln\left(R_i + \frac{y_3 - x_3}{\gamma_i}\right) - R_i \\ \text{for } x_3 < S(x_1, x_2) \text{ with } C_{\text{pn}}(x_1, x_2) \leqslant 0; \text{or } C_{\text{pn}}(x_1, x_2) > 0 \end{cases} \quad (8)$$

in which

$$R_i(\mathbf{y};\mathbf{x}) = \sqrt{(y_1 - x_1)^2 + (y_2 - x_2)^2 + (y_3 - x_3)^2/\gamma_i^2} \quad (9)$$

Some basic properties of the potential function χ_i are shown as follows

$$\gamma_i^2\frac{\partial^2\chi_i}{\partial y_3^2} = -\left(\frac{\partial^2}{\partial y_1^2} + \frac{\partial^2}{\partial y_2^2}\right)\chi_i \quad (10a)$$

$$\gamma_i^2\frac{\partial^2\chi_i}{\partial y_3^2} = \frac{1}{R_i} \quad (10b)$$

We emphasize that, throughout this paper, multi-valued functions $\ln z$ and $\sqrt{z}$ take values in their own single-valued analytic branches which satisfy $-\pi < \text{Im}(\ln z) < \pi$ and $\text{Re}(\sqrt{z}) > 0$ with $-\pi < \arg(z) < \pi$ respectively, where "Re" or "Im" denotes the real or imaginary part of a complex number, and "arg" means its argument.

Under the above preliminaries, we now begin our simple derivation. Firstly, substitution of Eq. (2) into Eq. (1) gives

$$u_m(\mathbf{x}) = -\int_A \begin{bmatrix} a_1 b_\beta \frac{\partial u_{\alpha m}}{\partial y_\alpha}\mathrm{d}A_\beta + a_2 b_\beta \frac{\partial u_{\beta m}}{\partial y_\alpha}\mathrm{d}A_\alpha + a_2 b_\beta \frac{\partial u_{\alpha m}}{\partial y_\beta}\mathrm{d}A_\alpha \\ +(a_1 + a_4) b_\beta \frac{\partial u_{3m}}{\partial y_3}\mathrm{d}A_\beta + (a_2 + a_5) b_\beta \frac{\partial u_{\beta m}}{\partial y_3}\mathrm{d}A_3 \\ +(a_2 + a_5) b_\beta \frac{\partial u_{3m}}{\partial y_\beta}\mathrm{d}A_3 + (a_1 + a_4) b_3 \frac{\partial u_{\alpha m}}{\partial y_\alpha}\mathrm{d}A_3 \\ +(a_2 + a_5) b_3 \frac{\partial u_{3m}}{\partial y_\alpha}\mathrm{d}A_\alpha + (a_2 + a_5) b_3 \frac{\partial u_{\alpha m}}{\partial y_3}\mathrm{d}A_\alpha \\ +(a_1 + 2a_2 + a_3 + 2a_4 + 4a_5) b_3 \frac{\partial u_{3m}}{\partial y_3}\mathrm{d}A_3 \end{bmatrix} \quad (11)$$

Then substituting Eq. (4) into Eq. (11), and utilizing the Stokes' theorem

$$\int_A (\mathrm{d}A_i\frac{\partial\phi}{\partial x_j} - \mathrm{d}A_j\frac{\partial\phi}{\partial x_i}) = \varepsilon_{ijk}\oint_C \phi\,\mathrm{d}x_k \quad (12)$$

together with the symmetry properties of the Green's tensor in a full space

$$u_{ij}(\mathbf{y};\mathbf{x}) = u_{ij}(\mathbf{x};\mathbf{y}) = u_{ji}(\mathbf{y};\mathbf{x}) \ \text{ or } \ \frac{\partial}{\partial y_i} = -\frac{\partial}{\partial x_i} \quad (13)$$

we finally obtain the displacement field of a simple dislocation loop as

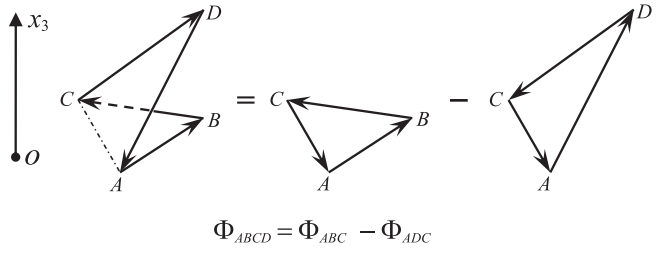

Fig. 2. A complex dislocation loop *ABCD* which can be decomposed into two triangular simple dislocation loops *ABC* and *ADC*. In this special case, Φ_{ABCD} is a linear superposition of Φ_{ABC} and Φ_{ADC}, both of which can be easily determined by Eq. (30).

$$u_\xi(\mathbf{x}) = -\frac{b_\xi}{4\pi}\Omega_3 - \frac{1}{4\pi}\oint_C (b_\beta \varepsilon_{\xi\beta 3} \mathrm{d}y_3 + \gamma_3^2 b_3 \varepsilon_{\xi 3\kappa} \mathrm{d}y_\kappa) \frac{\partial^2(\gamma_3\chi_3)}{\partial y_3^2} + \frac{1}{4\pi}\frac{\partial}{\partial x_\xi}\oint_C \left[b_\beta \varepsilon_{\alpha\beta 3} \frac{2}{\gamma_3^2} \frac{\partial(f_i\gamma_i\chi_i)}{\partial y_\alpha} \mathrm{d}y_3 + b_\beta \varepsilon_{3\beta\kappa} \frac{\partial(g_i\gamma_i\chi_i)}{\partial y_3} \mathrm{d}y_\kappa + b_3 \varepsilon_{\alpha 3\kappa} \frac{\partial(g_i\gamma_i\chi_i)}{\partial y_\alpha} \mathrm{d}y_\kappa \right] \tag{14a}$$

and

$$u_3(\mathbf{x}) = -\frac{b_3}{4\pi} m_\eta g_\eta \Omega_\eta - \frac{1}{4\pi}\oint_C b_\beta \varepsilon_{3\beta\kappa} \frac{\partial^2(m_\eta g_\eta \gamma_\eta \chi_\eta)}{\partial y_3^2} \mathrm{d}y_\kappa + \frac{1}{4\pi}\frac{\partial}{\partial x_3}\oint_C b_\beta \varepsilon_{\alpha\beta 3} \frac{2}{\gamma_3^2} \frac{\partial(m_\eta f_\eta \gamma_\eta \chi_\eta)}{\partial y_\alpha} \mathrm{d}y_3 \tag{14b}$$

where each line integral is along the dislocation loop following the positive direction, ε_{ijk} is the permutation tensor, and the coefficients f_i, g_i are defined in Eq. (25) of Section 4. In the above derivation, use has been made of the variants of Eq. (5) for further simplification,

$$\begin{aligned} &(a_2 + a_5) = a_2\gamma_3^2 \\ &(a_1 + a_2 + a_4 + a_5)m_\alpha + (a_2 + a_5) = (a_1 + 2a_2)\gamma_\alpha^2 \\ &(a_1 + 2a_2 + a_3 + 2a_4 + 4a_5)m_\alpha - (a_1 + a_2 + a_4 + a_5)\gamma_\alpha^2 \\ &\quad = (a_2 + a_5)m_\alpha\gamma_\alpha^2 \end{aligned} \tag{15}$$

Also in Eqs. (14a,b), Ω_i is defined by an area integral over the dislocation surface or a line integral along the dislocation loop as

$$\Omega_i(\mathbf{x}) = \int_A (\mathrm{d}A_\alpha \frac{\partial}{\partial y_\alpha} + \gamma_i^2 \mathrm{d}A_3 \frac{\partial}{\partial y_3}) \frac{\partial^2(\gamma_i\chi_i)}{\partial y_3^2} \tag{16a}$$

or

$$\Omega_i(\mathbf{x}) = \int_A (\mathrm{d}A_\alpha \frac{\partial}{\partial y_3} - \mathrm{d}A_3 \frac{\partial}{\partial y_\alpha}) \frac{\partial^2(\gamma_i\chi_i)}{\partial y_\alpha \partial y_3} = \oint_C \varepsilon_{\beta 3\kappa} \frac{\partial^2(\gamma_i\chi_i)}{\partial y_\beta \partial y_3} \mathrm{d}y_\kappa \tag{16b}$$

Eqs. (10a) and (12) contribute to the derivation of Eq. (16b). Analogous to the traditional solid angle, here we call Ω_i the *quasi solid angle*, which contributes to the displacement discontinuities over the dislocation surface, whilst other line-integral terms in Eqs. (14a,b) are continuous except on the dislocation line.

Eqs. (14a,b) are the main results of this paper, which have never appeared in the literature to the best of our knowledge, and will form the basis of later sections.

According to Ding et al. (2006), there are only three possible cases for the values of γ_α, i.e., (i) $\gamma_1 > 0$, $\gamma_2 > 0$, $\gamma_1 \neq \gamma_2$; (ii) $\mathrm{Re}(\gamma_1) > 0$, $\mathrm{Im}(\gamma_1) \neq 0$, $\bar{\gamma}_1 = \gamma_2$; (iii) $\gamma_1 = \gamma_2 > 0$, where an over-bar denotes the complex conjugate. It should be pointed out that Eqs. (14a,b) are applicable to cases (i) and (ii). The degenerate case (iii) will be considered in the next section.

3. Reduction to the Burgers displacement equation

Eqs. (14a,b) can be reduced to the well-known Burgers displacement equation of dislocation loops in an isotropic full space. To do this, it is convenient to transform Eqs. (14a,b) into the following form

$$\begin{aligned} u_\xi(\mathbf{x}) = &-\frac{b_\xi}{4\pi}\Omega_3 - \frac{1}{4\pi}\oint_C (b_\beta \varepsilon_{\xi\beta k} + \gamma_3^2 b_3 \varepsilon_{\xi 3k}) \frac{\partial^2(\gamma_3\chi_3)}{\partial y_3^2} \mathrm{d}y_k \\ &+ \frac{1}{4\pi}\frac{m_1}{\Theta}\frac{2}{\gamma_3^2}\frac{\partial}{\partial x_\xi}\oint_C b_j \varepsilon_{ijk}\frac{\partial}{\partial y_i}\frac{\gamma_1\chi_1 - \gamma_2\chi_2}{\gamma_1 - \gamma_2}\mathrm{d}y_k \\ &+ \frac{1}{4\pi}\frac{m_1}{\Theta}\left(m_2 + 1 - \frac{2}{\gamma_3^2}\right)\frac{\partial}{\partial x_\xi}\oint_C \left(b_\beta \varepsilon_{3\beta\kappa}\frac{\partial}{\partial y_3} + b_3 \varepsilon_{\alpha 3\kappa}\frac{\partial}{\partial y_\alpha}\right) \\ &\frac{\gamma_1\chi_1 - \gamma_2\chi_2}{\gamma_1 - \gamma_2}\mathrm{d}y_\kappa + \frac{1}{4\pi}\frac{\partial}{\partial x_\xi}\oint_C \left(b_\beta \varepsilon_{\alpha\beta 3}\frac{2}{\gamma_3^2}\frac{\partial}{\partial y_\alpha}\mathrm{d}y_3 \right. \\ &\left. + b_\beta \varepsilon_{3\beta\kappa}\frac{\partial}{\partial y_3}\mathrm{d}y_\kappa + b_3 \varepsilon_{\alpha 3\kappa}\frac{\partial}{\partial y_\alpha}\mathrm{d}y_\kappa\right)(\gamma_3\chi_3 - \gamma_1\chi_1) \end{aligned} \tag{17a}$$

and

$$\begin{aligned} u_3(\mathbf{x}) = &-\frac{b_3}{4\pi}\Omega_1 - \frac{1}{4\pi}\oint_C b_j \varepsilon_{3jk}\frac{\partial^2(\gamma_1\chi_1)}{\partial y_3^2}\mathrm{d}y_k + \frac{1}{4\pi}\frac{1}{\Theta}\frac{2}{\gamma_3^2}\frac{\partial}{\partial x_3} \\ &\oint_C b_j \varepsilon_{ijk}\frac{\partial}{\partial y_i}\frac{\gamma_1\chi_1 - \gamma_2\chi_2}{\gamma_1 - \gamma_2}\mathrm{d}y_k + \frac{1}{4\pi}\frac{1}{\Theta}\left(m_2 + 1 - \frac{2}{\gamma_3^2}\right)\frac{\partial}{\partial x_3} \\ &\oint_C \left(b_\beta \varepsilon_{3\beta\kappa}\frac{\partial}{\partial y_3} + b_3 \varepsilon_{\alpha 3\kappa}\frac{\partial}{\partial y_\alpha}\right)\frac{\gamma_1\chi_1 - \gamma_2\chi_2}{\gamma_1 - \gamma_2}\mathrm{d}y_\kappa \end{aligned} \tag{17b}$$

where use has been made of the following relation (Fabrikant, 2004)

$$m_1 - m_2 = \Theta(\gamma_1 - \gamma_2); \quad \Theta = c_{11}(\gamma_1 + \gamma_2)/(c_{13} + c_{44}) \tag{18}$$

We now consider the case of multiple roots in Eq. (6). When $m_1 \to m_2 \to m_0$, or $\gamma_1 \to \gamma_2 \to \gamma_0$, we obtain

$$\begin{aligned} &\lim_{\gamma_1\to\gamma_2\to\gamma_0}\frac{\gamma_1\chi_1 - \gamma_2\chi_2}{\gamma_1 - \gamma_2} = \frac{\partial(\gamma_0\chi_0)}{\partial\gamma_0} = -R_0; \\ &\lim_{\gamma_1\to\gamma_2\to\gamma_0}\Theta = \Theta_0 = \frac{2c_{11}\gamma_0}{(c_{13} + c_{44})} \end{aligned} \tag{19}$$

where χ_0 and R_0 are defined in Eqs. (8) and (9), with the index "0" in place of "i" there.

Substitution of Eq. (19) into Eqs. (17a,b) gives

$$\begin{aligned} u_\xi(\mathbf{x}) = &-\frac{b_\xi}{4\pi}\Omega_3 - \frac{1}{4\pi}\oint_C \frac{b_\beta \varepsilon_{\xi\beta k} + \gamma_3^2 b_3 \varepsilon_{\xi 3k}}{\gamma_3 R_3}\mathrm{d}y_k + \frac{1}{4\pi}\frac{m_0}{\Theta_0}\frac{2}{\gamma_3^2}\frac{\partial}{\partial x_\xi} \\ &\oint_C b_j \varepsilon_{jik}\frac{\partial R_0}{\partial y_i}\mathrm{d}y_k + \frac{1}{4\pi}\frac{m_0}{\Theta_0}\left(m_0 + 1 - \frac{2}{\gamma_3^2}\right)\frac{\partial}{\partial x_\xi} \\ &\oint_C \left(b_\beta \varepsilon_{\beta 3\kappa}\frac{\partial R_0}{\partial y_3}\mathrm{d}y_\kappa + b_3 \varepsilon_{3\alpha\kappa}\frac{\partial R_0}{\partial y_\alpha}\mathrm{d}y_\kappa\right) + \frac{1}{4\pi}\frac{\partial}{\partial x_\xi} \\ &\oint_C \left(b_\beta \varepsilon_{\alpha\beta 3}\frac{2}{\gamma_3^2}\frac{\partial}{\partial y_\alpha}\mathrm{d}y_3 + b_\beta \varepsilon_{3\beta\kappa}\frac{\partial}{\partial y_3}\mathrm{d}y_\kappa + b_3 \varepsilon_{\alpha 3\kappa}\frac{\partial}{\partial y_\alpha}\mathrm{d}y_\kappa\right) \\ &(\gamma_3\chi_3 - \gamma_0\chi_0) \end{aligned} \tag{20a}$$

and

$$\begin{aligned} u_3(\mathbf{x}) = &-\frac{b_3}{4\pi}\Omega_0 - \frac{1}{4\pi}\oint_C \frac{b_j \varepsilon_{3jk}}{\gamma_0 R_0}\mathrm{d}y_k + \frac{1}{4\pi}\frac{1}{\Theta_0}\frac{2}{\gamma_3^2}\frac{\partial}{\partial x_3}\oint_C b_j \varepsilon_{jik} \\ &\times \frac{\partial R_0}{\partial y_i}\mathrm{d}y_k + \frac{1}{4\pi}\frac{1}{\Theta_0}\left(m_0 + 1 - \frac{2}{\gamma_3^2}\right)\frac{\partial}{\partial x_3} \\ &\oint_C \left(b_\beta \varepsilon_{\beta 3\kappa}\frac{\partial R_0}{\partial y_3}\mathrm{d}y_\kappa + b_3 \varepsilon_{3\alpha\kappa}\frac{\partial R_0}{\partial y_\alpha}\mathrm{d}y_\kappa\right) \end{aligned} \tag{20b}$$

where Ω_0 is defined in Eqs. (16a,b), again, with the index "0" in place of "i" there. Eqs. (20a,b) give the displacement field for the degenerate case of $\gamma_1 = \gamma_2 > 0$.

For isotropic materials, we have

$$m_0 = 1; \quad \gamma_3 = \gamma_0 = 1; \quad R_3 = R_0; \quad \chi_3 = \chi_0 \tag{21}$$

By virtue of Eq. (21), Eq. (20a,b) can be reduced exactly to the Burgers displacement equation (Hirth and Lothe, 1982).

4. Stress field due to a simple dislocation loop

The dislocation-induced stresses can be derived from Eqs. (14a,b) by virtue of the following stress-displacement relations

$$\sigma_{ij}(\mathbf{x}) = c_{ijkl}\frac{\partial u_k(\mathbf{x})}{\partial x_l} \tag{22}$$

Thus, we need to calculate the spatial derivatives of the quasi solid angle Ω_i as follows

$$\frac{\partial \Omega_i(\mathbf{x})}{\partial x_j} = -\int_A \left(\mathrm{d}A_\alpha \frac{\partial}{\partial y_\alpha} + \gamma_i^2 \mathrm{d}A_3 \frac{\partial}{\partial y_3}\right) \frac{\partial}{\partial y_j} \frac{\partial^2(\gamma_i \chi_i)}{\partial y_3^2}$$
$$= \int_A \left(\mathrm{d}A_j \frac{\partial}{\partial y_\alpha} - \mathrm{d}A_\alpha \frac{\partial}{\partial y_j}\right) \frac{\partial}{\partial y_\alpha} \frac{\partial^2(\gamma_i \chi_i)}{\partial y_3^2}$$
$$+ \gamma_i^2 \left(\mathrm{d}A_j \frac{\partial}{\partial y_3} - \mathrm{d}A_3 \frac{\partial}{\partial y_j}\right) \frac{\partial}{\partial y_3} \frac{\partial^2(\gamma_i \chi_i)}{\partial y_3^2}$$
$$= \oint_C \left(\varepsilon_{j\alpha k} \frac{\partial}{\partial y_\alpha} + \gamma_i^2 \varepsilon_{j3k} \frac{\partial}{\partial y_3}\right) \frac{\partial^2(\gamma_i \chi_i)}{\partial y_3^2} \mathrm{d}y_k \tag{23}$$

where use has been made of Eqs. (10a), (12), and (13) in the derivation.

After some lengthy derivations, the final results for the stress field of a simple dislocation loop are found to be

$$\sigma_{\xi\eta}(\mathbf{x}) = \frac{c_{44}}{4\pi} \delta_{\xi\eta} \oint_C \begin{bmatrix} b_\beta \varepsilon_{\alpha\beta 3} \frac{2}{\gamma_3^2} \frac{\partial}{\partial y_\alpha} \frac{\partial^2}{\partial y_3^2} \left(\frac{2}{\gamma_3^2} f_i \gamma_i^3 \chi_i - g_i \gamma_i \chi_i\right) \mathrm{d}y_3 \\ + b_\beta \varepsilon_{3\beta\kappa} \frac{\partial}{\partial y_3} \frac{\partial^2}{\partial y_3^2} \left(\frac{2}{\gamma_3^2} g_\alpha \gamma_\alpha^3 \chi_\alpha - h_\alpha \gamma_\alpha \chi_\alpha\right) \mathrm{d}y_\kappa \\ - b_3 \varepsilon_{\alpha 3\kappa} \frac{\partial}{\partial y_\alpha} \frac{\partial^2(h_\beta \gamma_\beta \chi_\beta)}{\partial y_3^2} \mathrm{d}y_\kappa \end{bmatrix}$$
$$+ \frac{c_{44}}{4\pi} \frac{2}{\gamma_3^2} \oint_C \begin{bmatrix} b_\beta \varepsilon_{\alpha\beta 3} \frac{2}{\gamma_3^2} \frac{\partial}{\partial y_\alpha} \frac{\partial^2(f_i \gamma_i \chi_i)}{\partial y_\xi \partial y_\eta} \mathrm{d}y_3 + b_\beta \varepsilon_{3\beta\kappa} \frac{\partial}{\partial y_3} \frac{\partial^2(g_i \gamma_i \chi_i)}{\partial y_\xi \partial y_\eta} \mathrm{d}y_\kappa \\ + \frac{1}{2}(b_\xi \varepsilon_{\eta\kappa 3} + b_\eta \varepsilon_{\xi\kappa 3}) \frac{\partial}{\partial y_3} \frac{\partial^2(\gamma_3^3 \chi_3)}{\partial y_3^2} \mathrm{d}y_\kappa \\ + \frac{1}{2} b_3 (\varepsilon_{\alpha\xi 3} \frac{\partial}{\partial y_\eta} + \varepsilon_{\alpha\eta 3} \frac{\partial}{\partial y_\xi}) \frac{\partial^2(g_i \gamma_i \chi_i)}{\partial y_\alpha \partial y_3} \mathrm{d}y_3 \\ + \frac{1}{2} b_3 (\varepsilon_{\alpha 3\eta} \mathrm{d}y_\xi + \varepsilon_{\alpha 3\xi} \mathrm{d}y_\eta) \frac{\partial}{\partial y_\alpha} \frac{\partial^2(g_\beta \gamma_\beta^3 \chi_\beta)}{\partial y_3^2} \end{bmatrix} \tag{24a}$$

and

$$\sigma_{\xi 3}(\mathbf{x}) = \frac{c_{44}}{4\pi} \oint_C \begin{bmatrix} b_\beta \varepsilon_{\alpha\beta 3} \frac{2}{\gamma_3^2} \frac{\partial}{\partial y_\alpha} \frac{\partial^2(g_i \gamma_i \chi_i)}{\partial y_\xi \partial y_3} \mathrm{d}y_3 + b_\beta \varepsilon_{3\beta\kappa} \frac{\partial}{\partial y_\xi} \frac{\partial^2(h_\alpha \gamma_\alpha \chi_\alpha)}{\partial y_3^2} \mathrm{d}y_\kappa \\ + b_\beta \varepsilon_{\xi\beta 3} \frac{\partial}{\partial y_3} \frac{\partial^2(\gamma_3 \chi_3)}{\partial y_3^2} \mathrm{d}y_3 - b_\beta \varepsilon_{\alpha\beta 3} \frac{\partial}{\partial y_\alpha} \frac{\partial^2(\gamma_3 \chi_3)}{\partial y_3^2} \mathrm{d}y_\xi \\ + b_3 \varepsilon_{\alpha\xi 3} \frac{\partial}{\partial y_\alpha} \frac{\partial^2(h_i \gamma_i \chi_i)}{\partial y_3^2} \mathrm{d}y_3 + b_3 \varepsilon_{3\xi\kappa} \frac{\partial}{\partial y_3} \frac{\partial^2(h_\alpha \gamma_\alpha^3 \chi_\alpha)}{\partial y_3^2} \mathrm{d}y_\kappa \end{bmatrix} \tag{24b}$$

and

$$\sigma_{33}(\mathbf{x}) = \frac{c_{44}}{4\pi} \oint_C \begin{bmatrix} b_\beta \varepsilon_{\alpha\beta 3} \frac{2}{\gamma_3^2} \frac{\partial}{\partial y_\alpha} \frac{\partial^2(g_\eta \gamma_\eta^3 \chi_\eta)}{\partial y_3^2} \mathrm{d}y_3 + b_\beta \varepsilon_{3\beta\kappa} \frac{\partial}{\partial y_3} \frac{\partial^2(h_\eta \gamma_\eta^3 \chi_\eta)}{\partial y_3^2} \mathrm{d}y_\kappa \\ + b_3 \varepsilon_{\alpha 3\kappa} \frac{\partial}{\partial y_\alpha} \frac{\partial^2(h_\eta \gamma_\eta^3 \chi_\eta)}{\partial y_3^2} \mathrm{d}y_\kappa \end{bmatrix} \tag{24c}$$

where

$$\mathbf{f} = \{f_1, f_2, f_3\} = \left\{\frac{m_2}{m_1 - m_2}, \frac{m_1}{m_2 - m_1}, 1\right\}$$
$$\mathbf{g} = \{g_1, g_2, g_3\} = \left\{\frac{m_2+1}{m_1 - m_2}, \frac{m_1+1}{m_2 - m_1}, 1\right\} \tag{25}$$
$$\mathbf{h} = \{h_1, h_2, h_3\} = \left\{\frac{m_1+m_2+2}{m_1 - m_2}, \frac{m_1+m_2+2}{m_2 - m_1}, 1\right\}$$

When deriving Eqs. (24a,b), use has been made of the following identities (Hirth and Lothe, 1982)

$$\delta_{\xi\alpha}\varepsilon_{3\beta\kappa} + \delta_{\xi\beta}\varepsilon_{\alpha 3\kappa} = -\delta_{\xi\kappa}\varepsilon_{\alpha\beta 3}$$
$$\delta_{\eta\kappa}\varepsilon_{\alpha 3\xi} + \delta_{\xi\kappa}\varepsilon_{\alpha 3\eta} + \delta_{\xi\alpha}\varepsilon_{\eta 3\kappa} + \delta_{\eta\alpha}\varepsilon_{\xi 3\kappa} = 2\delta_{\xi\eta}\varepsilon_{\alpha 3\kappa} \tag{26}$$
$$\delta_{\xi\beta}\varepsilon_{\alpha\eta 3} + \delta_{\eta\beta}\varepsilon_{\alpha\xi 3} + \delta_{\eta\alpha}\varepsilon_{\xi\beta 3} + \delta_{\xi\alpha}\varepsilon_{\eta\beta 3} = 2\delta_{\eta\xi}\varepsilon_{\alpha\beta 3}$$

and Eqs. (27a,b) below

$$2\oint_C \varepsilon_{\alpha 3\kappa} \frac{\partial}{\partial y_\alpha} \frac{\partial^2(\gamma_i \chi_i)}{\partial y_\xi \partial y_\eta} \mathrm{d}y_\kappa + \oint_C \left(\varepsilon_{\xi 3\kappa} \frac{\partial}{\partial y_\eta} + \varepsilon_{\eta 3\kappa} \frac{\partial}{\partial y_\xi}\right) \frac{\partial^2(\gamma_i^3 \chi_i)}{\partial y_3^2} \mathrm{d}y_\kappa$$
$$= \oint_C \left(\varepsilon_{\beta\xi 3} \frac{\partial}{\partial y_\eta} + \varepsilon_{\beta\eta 3} \frac{\partial}{\partial y_\xi}\right) \frac{\partial^2(\gamma_i \chi_i)}{\partial y_\beta \partial y_3} \mathrm{d}y_3 \tag{27a}$$

$$\oint_C \varepsilon_{\alpha 3\kappa} \frac{\partial^2}{\partial y_\alpha \partial y_\xi} \frac{\partial(\gamma_i \chi_i)}{\partial y_3} \mathrm{d}y_\kappa + \oint_C \varepsilon_{\xi 3\kappa} \frac{\partial}{\partial y_3} \frac{\partial^2(\gamma_i^3 \chi_i)}{\partial y_3^2} \mathrm{d}y_\kappa$$
$$= \oint_C \varepsilon_{\beta\xi 3} \frac{\partial}{\partial y_\beta} \frac{\partial^2(\gamma_i \chi_i)}{\partial y_3^2} \mathrm{d}y_3 \tag{27b}$$

$$\oint_C \varepsilon_{\alpha 3\kappa} \frac{\partial^2(\gamma_i \chi_i)}{\partial y_\alpha \partial y_\xi} \mathrm{d}y_\kappa + \oint_C \varepsilon_{\xi 3\kappa} \frac{\partial^2(\gamma_i^3 \chi_i)}{\partial y_3^2} \mathrm{d}y_\kappa$$
$$= \oint_C \varepsilon_{\beta\xi 3} \frac{\partial^2(\gamma_i \chi_i)}{\partial y_\beta \partial y_3} \mathrm{d}y_3 \tag{27c}$$

Eqs. (27a–c) can be easily proved via Eqs. (10a) and (12). Eq. (27c) is needed in later derivation.

It can be verified that, in the transversely isotropic case, our stress formulae in Eqs. (24a–c) are simpler and more efficient than the Mura's formula (Hirth and Lothe, 1982) after substituting Eq. (4) into it. We also point out that a similar limiting process as in Section 3 can be followed if one is interested in the stress field for the degenerate case of $\gamma_1 = \gamma_2 > 0$.

We should keep in mind that, although the displacements and stresses in terms of line integrals over the closed dislocation loop have to satisfy the stress–displacement relations (22), their corresponding integrands do not necessarily satisfy such relations. In addition, Eqs. (27a–c) are generally valid for a "closed" loop, but may not be if otherwise. This implies the non-uniqueness of the integrands of the line integrals in Eqs. (14a,b) and (24a–c), and thus the non-uniqueness of the displacement and stress fields due to an "open" dislocation segment (see, e.g., Hirth and Lothe, 1982; Wang, 1996; Paynter et al., 2007; Yin et al., 2010). This issue will be further illustrated in Section 8.

In summary, Eqs. (14a,b) (Eqs. (20a,b) for the degenerate case) and Eqs. (24a–c) are, respectively, the displacement and stress fields induced by a simple Volterra dislocation loop of arbitrary shape with a constant Burgers vector in a transversely isotropic elastic full space. However, the derived solutions are expressed explicitly in terms of the potential functions χ_i defined in Eq. (8), which is only suitable for a simple dislocation loop. As such, we further simplify, clarify and generalize these solutions by eliminating χ_i in the next section.

5. Further simplification and generalization of the elastic field solution

For future applications, we now simplify the displacement field solution in Eqs. (14a,b) and the stress field solution in Eqs. (24a–c) by substituting those three potential functions χ_i as shown in Eq. (8). After some elementary calculations, we can write Eqs. (14a,b) and Eqs. (24a–c) concisely as

$$u_\xi(\mathbf{x}) = \frac{b_\xi}{4\pi}\left(\Phi + \frac{1}{\gamma_3}\varepsilon_{\alpha 3\kappa} \mathrm{I}^{\alpha 3}_{2;3\kappa}\right) + \frac{b_3}{4\pi}\left(\frac{g_i}{\gamma_i}\varepsilon_{\alpha\xi 3}\mathrm{I}^{\alpha 3}_{2;i3} + \gamma_\alpha g_\alpha \varepsilon_{\xi 3\kappa}\mathrm{I}^{\sim}_{0;\alpha\kappa}\right)$$
$$- \frac{b_\beta}{4\pi} \times \left\{\frac{2}{\gamma_3^2}\gamma_i f_i \left[\varepsilon_{\alpha\beta 3}\left(\frac{2}{\gamma_i^2}\mathrm{I}^{\xi\alpha 33}_{4;i3} + \mathrm{I}^{\xi\alpha}_{2;i3}\right) - \varepsilon_{\xi\beta 3}\left(\frac{1}{\gamma_i^2}\mathrm{I}^{33}_{2;i3} + \mathrm{I}^{\sim}_{0;i3}\right)\right]\right.$$
$$\left. + \frac{1}{\gamma_3}\varepsilon_{\xi\beta 3}\mathrm{I}^{\sim}_{0;33} - \frac{g_i}{\gamma_i}\varepsilon_{\beta 3\kappa}\mathrm{I}^{\xi 3}_{2;i\kappa}\right\} \tag{28a}$$

$$u_3(\mathbf{x}) = \frac{b_3}{4\pi}\left(\Phi + \frac{m_\eta g_\eta}{\gamma_\eta}\varepsilon_{\alpha 3\kappa}\mathrm{I}^{\alpha 3}_{2;\eta\kappa}\right)$$
$$+ \frac{b_\beta}{4\pi}\left(\frac{2}{\gamma_3^2}\frac{m_\eta f_\eta}{\gamma_\eta}\varepsilon_{\alpha\beta 3}\mathrm{I}^{\alpha 3}_{2;\eta 3} - \frac{m_\eta g_\eta}{\gamma_\eta}\varepsilon_{3\beta\kappa}\mathrm{I}^{\sim}_{0;\eta\kappa}\right) \tag{28b}$$

and

$$\sigma_{\xi\eta}(\mathbf{x}) = \frac{c_{44}}{4\pi}\delta_{\xi\eta}\begin{bmatrix} b_\beta \frac{2}{\gamma_3^2}\left(\frac{g_i}{\gamma_i} - \frac{2}{\gamma_3^2}\gamma_i f_i\right)\varepsilon_{\alpha\beta3}\mathrm{J}^{\alpha}_{0;i3} + b_\beta \frac{2}{\gamma_3^2}\frac{2}{\gamma_3^2}\gamma_i f_i \varepsilon_{\alpha\beta3}\left(\mathrm{I}^{\alpha}_{2;i3} + \frac{2}{\gamma_i^2}\mathrm{I}^{\alpha33}_{4;i3}\right) \\ -b_\beta\left(\frac{2}{\gamma_3^2}\frac{g_\alpha}{\gamma_\alpha} - \frac{1}{\gamma_\alpha^2}\frac{h_\alpha}{\gamma_\alpha}\right)\varepsilon_{3\beta\kappa}\mathrm{J}^{3}_{0;\alpha\kappa} - b_\beta \frac{2}{\gamma_3^2}\frac{g_i}{\gamma_i}\varepsilon_{3\beta\kappa}\mathrm{I}^{3}_{2;i\kappa} + b_3\frac{h_\beta}{\gamma_\beta}\varepsilon_{\alpha3\kappa}\mathrm{J}^{\alpha}_{0;\beta\kappa} \end{bmatrix}$$
$$+\frac{c_{44}}{4\pi}\frac{2}{\gamma_3^2}\begin{Bmatrix} b_\beta \frac{2}{\gamma_3^2}\gamma_i f_i \begin{bmatrix} \varepsilon_{\eta\beta3}\left(\mathrm{I}^{\xi}_{2;i3} + \frac{2}{\gamma_i^2}\mathrm{I}^{\xi33}_{4;i3}\right) + \varepsilon_{\xi\beta3}\left(\mathrm{I}^{\eta}_{2;i3} + \frac{2}{\gamma_i^2}\mathrm{I}^{\eta33}_{4;i3}\right) \\ +\varepsilon_{\alpha\beta3}\left(\mathrm{J}^{\alpha\xi\eta}_{2;i3} - 4\mathrm{I}^{\alpha\xi\eta}_{4;i3} - \frac{8}{\gamma_i^2}\mathrm{I}^{\alpha\xi\eta33}_{6;i3}\right) \end{bmatrix} \\ +b_\beta\frac{g_i}{\gamma_i}\varepsilon_{3\beta\kappa}\left(\mathrm{J}^{\xi\eta3}_{2;i\kappa} + 2\mathrm{I}^{\xi\eta3}_{4;i\kappa}\right) - \frac{1}{2}\frac{1}{\gamma_3}(b_\xi\varepsilon_{3\eta\kappa} + b_\eta\varepsilon_{3\xi\kappa})\mathrm{J}^{3}_{0;3\kappa} \\ +\frac{1}{2}b_3\frac{g_i}{\gamma_i}\left[\varepsilon_{\alpha\xi3}\left(\mathrm{J}^{\eta\alpha3}_{2;i3} + 2\mathrm{I}^{\eta\alpha3}_{4;i3}\right) + \varepsilon_{\alpha\eta3}\left(\mathrm{J}^{\xi\alpha3}_{2;i3} + 2\mathrm{I}^{\xi\alpha3}_{4;i3}\right)\right] \\ -\frac{1}{2}b_3\gamma_\beta g_\beta\left(\varepsilon_{\alpha3\eta}\mathrm{J}^{\alpha}_{0;\beta\xi} + \varepsilon_{\alpha3\xi}\mathrm{J}^{\alpha}_{0;\beta\eta}\right) \end{Bmatrix} \tag{29a}$$

$$\sigma_{\xi3}(\mathbf{x}) = -\frac{c_{44}b_3}{4\pi}\left(\frac{h_i}{\gamma_i}\varepsilon_{\alpha\xi3}\mathrm{J}^{\alpha}_{0;i3} + \frac{h_\alpha}{\gamma_\alpha}\varepsilon_{3\xi\kappa}\mathrm{J}^{3}_{0;\alpha\kappa}\right)$$
$$-\frac{c_{44}b_\beta}{4\pi}\left\{\frac{2}{\gamma_3^2}\frac{g_i}{\gamma_i}\left[\varepsilon_{\xi\beta3}\mathrm{I}^{3}_{2;i3} - \varepsilon_{\alpha\beta3}\left(\mathrm{J}^{\xi\alpha3}_{2;i3} + 2\mathrm{I}^{\xi\alpha3}_{4;i3}\right)\right]\right.$$
$$\left.+\frac{h_\alpha}{\gamma_\alpha}\varepsilon_{3\beta\kappa}\mathrm{J}^{\xi}_{0;\alpha\kappa} + \frac{1}{\gamma_3}\left(\frac{1}{\gamma_3^2}\varepsilon_{\xi\beta3}\mathrm{J}^{3}_{0;33} - \varepsilon_{\alpha\beta3}\mathrm{J}^{\alpha}_{0;3\xi}\right)\right\} \tag{29b}$$

$$\sigma_{33}(\mathbf{x}) = -\frac{c_{44}b_3}{4\pi}\gamma_\eta h_\eta \varepsilon_{\alpha3\kappa}\mathrm{J}^{\alpha}_{0;\eta\kappa}$$
$$-\frac{c_{44}b_\beta}{4\pi}\left(\frac{2}{\gamma_3^2}\gamma_\eta g_\eta \varepsilon_{\alpha\beta3}\mathrm{J}^{\alpha}_{0;\eta3} + \frac{h_\eta}{\gamma_\eta}\varepsilon_{\beta\kappa3}\mathrm{J}^{3}_{0;\eta\kappa}\right) \tag{29c}$$

where the coefficients f_i, g_i and h_i are defined the same as those in Eq. (25), and

$$\Phi(\mathbf{x}) = \mathrm{sgn}\langle S(x_1,x_2) - x_3\rangle \varepsilon_{3\alpha\kappa}\oint_C \frac{(y_\alpha - x_\alpha)}{r_{\mathrm{pn}}^2}\mathrm{d}y_\kappa$$
$$= \mathrm{sgn}\langle S(x_1,x_2) - x_3\rangle \oint_C \mathrm{d}\arctan\frac{y_2 - x_2}{y_1 - x_1}$$
$$= \pi[1 - \mathrm{sgn}\langle C_{\mathrm{pn}}(x_1,x_2)\rangle]\mathrm{sgn}\langle S(x_1,x_2) - x_3\rangle \tag{30}$$

in which $S(x_1,x_2)$ and $C_{\mathrm{pn}}(x_1,x_2)$ are defined in Eq. (7) and also illustrated in Fig. 1, and $\mathrm{sgn}\langle x\rangle$ is the sign function, and

$$r_{\mathrm{pn}}(y_\alpha;x_\beta) = \sqrt{(y_1 - x_1)^2 + (y_2 - x_2)^2} \tag{31}$$

Also in Eqs. (28a)–(29c),

$$\overbrace{\mathrm{I}^{ij\cdots}_{N;mk}}^{M}(\mathbf{x}) = \oint_C \frac{\overbrace{(y_i - x_i)(y_j - x_j)\cdots}^{M}}{r_{\mathrm{pn}}^N R_m}\mathrm{d}y_k \text{ with } N = 0,2,4,6;\ M \le N,\ M \in \mathbb{N}$$
$$\overbrace{\mathrm{J}^{ij\cdots}_{N;mk}}^{M}(\mathbf{x}) = \oint_C \frac{\overbrace{(y_i - x_i)(y_j - x_j)\cdots}^{M}}{r_{\mathrm{pn}}^N R_m^3}\mathrm{d}y_k \text{ with } N = 0,2;\ M \le N+1,\ M \in \mathbb{N}$$
$$\mathrm{I}^{\sim}_{N;mk}(\mathbf{x}) = \oint_C \frac{1}{r_{\mathrm{pn}}^N R_m}\mathrm{d}y_k;\quad \mathrm{J}^{\sim}_{N;mk}(\mathbf{x}) = \oint_C \frac{1}{r_{\mathrm{pn}}^N R_m^3}\mathrm{d}y_k \tag{32}$$

We further point out that in the derivation of Eq. (28a), use has been made of the relation (27c).

Thus, by eliminating the three potential functions χ_i from Eqs. (14a,b) and Eqs. (24a–c), we have achieved an alternative yet more explicit solution of the elastic field due to a simple dislocation loop, as given in Eqs. (28a)–(29c).

It is observed from Eqs. (28a,b) and Eq. (30) that, for a simple dislocation loop of Type-I described by Eq. (7), the displacement discontinuities over the dislocation surface are totally attributed to the function Φ, which is extracted from the quasi solid angle Ω_i, i.e.,

$$\Omega_i = -\Phi - \varepsilon_{\alpha3\kappa}\mathrm{I}^{\alpha3}_{2;i\kappa}/\gamma_i \tag{33}$$

However, for a simple dislocation loop of Type-II, we can see that $\Phi = 0$, and thus it is the other part on the right hand side of Eq. (33) that contributes to the displacement discontinuities over the dislocation surface.

Moreover, we emphasize that, in Eqs. (28a,b), the function Φ defined in Eq. (30) is the only term which depends upon the configuration of the dislocation surface bounded by the dislocation loop. Therefore, we can conclude that: (i) the stress field solutions (29a–c) are generally valid for an arbitrary dislocation loop, whether simple or complex; (ii) the displacement field solutions (28a,b) are also applicable to a complex dislocation loop, provided that one can express function Φ of this complex loop as a superposition of functions Φ's of its constituent simple-loops (see Fig. 2 for example). This is feasible due to the existing simple and explicit form of Eq. (30) for a simple dislocation surface.

The function Φ we introduced possesses certain attractive features and it can be very convenient in analyzing the dislocation-induced elastic field. As an illustration, let us consider an assembly of simple and complex dislocation loops. We introduce a finite cylinder which is parallel to the x_3-axis and just contains all the dislocation surfaces in it, with its top on the plane $x_3 = x_{3\max}$ and its bottom on the plane $x_3 = x_{3\min}$ and its side on the cylindrical surface $F(x_1,x_2) = 0$, as shown in Fig. 3. Based upon the principle of superposition, function Φ makes no contribution to the displacement field outside the cylindrical surface (i.e., $F(x_1,x_2) > 0$ in Fig. 3). However, it is not the case inside the cylindrical surface (i.e., $F(x_1,x_2) < 0$). For example, for all the field points above the top (or similarly below the bottom) which lie on a line parallel to the x_3-axis, function Φ contributes a constant $2n\pi$ to the displacements, with n being some integer. Furthermore, it can be easily proved that, at infinity, the quasi solid angles become zero. Due to the above facts, we can derive an alternative expression for Φ from Eq. (33) as

$$\Phi(x_3 > x_{3\max}) = \lim_{x_3\to+\infty}(-\Omega_i - \varepsilon_{\alpha3\kappa}\mathrm{I}^{\alpha3}_{2;i\kappa}/\gamma_i) = -\varepsilon_{3\alpha\kappa}\oint_C \frac{(y_\alpha - x_\alpha)}{r_{\mathrm{pn}}^2}\mathrm{d}y_\kappa$$
$$\Phi(x_3 < x_{3\min}) = \lim_{x_3\to-\infty}(-\Omega_i - \varepsilon_{\alpha3\kappa}\mathrm{I}^{\alpha3}_{2;i\kappa}/\gamma_i) = +\varepsilon_{3\alpha\kappa}\oint_C \frac{(y_\alpha - x_\alpha)}{r_{\mathrm{pn}}^2}\mathrm{d}y_\kappa \tag{34}$$

It can be seen that the function Φ given in Eq. (34) is now independent of the configuration of the dislocation surface, whether simple or not; and it actually applies to all the field points outside the finite cylinder. We can thus conclude from Eqs. (28a,b) and (34) that, the closed dislocation lines themselves totally determine the induced displacement field outside the finite cylinder which is parallel to the x_3-axis and circumscribes the dislocation-loop assembly.

As an immediate application of our general elastic field solutions (28a)–(29c), we now consider a planar dislocation loop of arbitrary shape which is parallel to the plane of isotropy and lies on the plane $x_3 = x_{3\mathrm{const}}$. In this special case, Eqs. (28a)–(29c) can be considerably simplified to

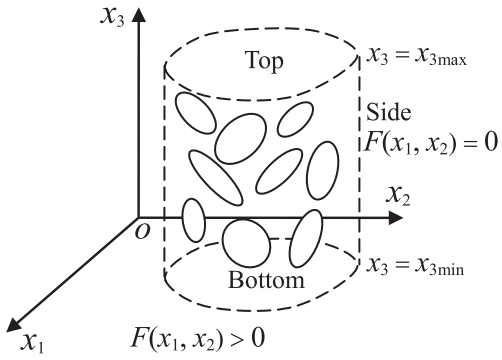

Fig. 3. An assembly of simple and complex dislocation loops which is circumscribed by a finite cylinder parallel to the x_3-axis.

$$u_\xi(\mathbf{x}) = \frac{b_3}{4\pi}\gamma_\alpha g_\alpha \varepsilon_{\xi 3\kappa}\tilde{\mathrm{I}}^{}_{0;\alpha\kappa} + \frac{b_\xi}{4\pi}\left[\Phi + \frac{1}{\gamma_3}(x_{3\mathrm{const}} - x_3)\varepsilon_{\alpha 3\kappa}\mathrm{I}^{\alpha}_{2;3\kappa}\right] + \frac{b_\beta}{4\pi}(x_{3\mathrm{const}} - x_3)\frac{g_i}{\gamma_i}\varepsilon_{3\beta\kappa}\mathrm{I}^{\xi}_{2;i\kappa} \tag{35a}$$

$$u_3(\mathbf{x}) = \frac{b_3}{4\pi}\left[\Phi + (x_{3\mathrm{const}} - x_3)\frac{m_\eta g_\eta}{\gamma_\eta}\varepsilon_{\alpha 3\kappa}\mathrm{I}^{\alpha}_{2;\eta\kappa}\right] - \frac{b_\beta}{4\pi}\frac{m_\eta g_\eta}{\gamma_\eta}\varepsilon_{3\beta\kappa}\tilde{\mathrm{I}}^{}_{0;\eta\kappa} \tag{35b}$$

and

$$\sigma_{\xi\eta}(\mathbf{x}) = -\frac{c_{44}}{4\pi}\delta_{\xi\eta}\begin{bmatrix} b_\beta(x_{3\mathrm{const}} - x_3)\left(\frac{2}{\gamma_3^2}\frac{g_\alpha}{\gamma_\alpha} - \frac{1}{\gamma_\alpha^2}\frac{h_\alpha}{\gamma_\alpha}\right)\varepsilon_{3\beta\kappa}\tilde{\mathrm{J}}^{}_{0;\alpha\kappa} \\ +b_\beta(x_{3\mathrm{const}} - x_3)\frac{2}{\gamma_3^2}\frac{g_i}{\gamma_i}\varepsilon_{3\beta\kappa}\tilde{\mathrm{I}}^{}_{2;i\kappa} - b_3\frac{h_\beta}{\gamma_\beta}\varepsilon_{\alpha 3\kappa}\mathrm{J}^{\alpha}_{0;\beta\kappa}\end{bmatrix} + \frac{c_{44}}{4\pi}\frac{2}{\gamma_3^2}\begin{bmatrix} b_\beta(x_{3\mathrm{const}} - x_3)\frac{g_i}{\gamma_i}\varepsilon_{3\beta\kappa}\left(\mathrm{J}^{\xi\eta}_{2;i\kappa} + 2\mathrm{I}^{\xi\eta}_{4;i\kappa}\right) \\ -\frac{1}{2}\frac{1}{\gamma_3}(x_{3\mathrm{const}} - x_3)(b_\xi\varepsilon_{3\eta\kappa} + b_\eta\varepsilon_{3\xi\kappa})\tilde{\mathrm{J}}^{}_{0;3\kappa} \\ -b_3\gamma_\beta g_\beta(\varepsilon_{\alpha 3\eta}\mathrm{J}^{\alpha}_{0;\beta\xi} + \varepsilon_{\alpha 3\xi}\mathrm{J}^{\alpha}_{0;\beta\eta})/2\end{bmatrix} \tag{36a}$$

$$\sigma_{\xi 3}(\mathbf{x}) = -\frac{c_{44}b_3}{4\pi}(x_{3\mathrm{const}} - x_3)\frac{h_\alpha}{\gamma_\alpha}\varepsilon_{3\xi\kappa}\tilde{\mathrm{J}}^{}_{0;\alpha\kappa} + \frac{c_{44}b_\beta}{4\pi}\left(\frac{1}{\gamma_3}\varepsilon_{\alpha\beta 3}\mathrm{J}^{\alpha}_{0;3\xi} - \frac{h_\alpha}{\gamma_\alpha}\varepsilon_{3\beta\kappa}\mathrm{J}^{\xi}_{0;\alpha\kappa}\right) \tag{36b}$$

$$\sigma_{33}(\mathbf{x}) = -\frac{c_{44}b_3}{4\pi}\gamma_\eta h_\eta \varepsilon_{\alpha 3\kappa}\mathrm{J}^{\alpha}_{0;\eta\kappa} - \frac{c_{44}b_\beta}{4\pi}(x_{3\mathrm{const}} - x_3)\frac{h_\eta}{\gamma_\eta}\varepsilon_{3\beta\kappa}\tilde{\mathrm{J}}^{}_{0;\eta\kappa} \tag{36c}$$

where Φ takes the following simple form via Eq. (30)

$$\Phi(\mathbf{x}) = \pi[1 - \mathrm{sgn}\langle C_{\mathrm{pn}}(x_1, x_2)\rangle]\mathrm{sgn}\langle x_{3\mathrm{const}} - x_3\rangle \tag{37}$$

It can be easily shown that, Eqs. (35a)–(36c) are mathematically identical to those derived by Tupholme (1974), and that our solutions are more explicit. Particularly, in our Eqs. (35a,b), the terms accounting for displacement discontinuities over the dislocation surface are separated naturally from the regular parts. If the dislocation loop is a circular one, then Eqs. (35a)–(36c) can be integrated analytically in terms of complete elliptic integrals, as will be shown in Section 7.

6. Elastic fields due to a straight dislocation segment of arbitrary orientation

We now consider a directional straight dislocation segment AB which begins at A (x_{1A}, x_{2A}, x_{3A}) and ends at B (x_{1B}, x_{2B}, x_{3B}). We express AB in terms of a parameter t as

$$x_i = x_{iA} + (x_{iB} - x_{iA})t, \quad t \in [0, 1] \tag{38}$$

Without loss of generality, we assume that AB lies on a closed simple dislocation loop C generally defined in Eq. (7), and goes along the positive direction of this loop.

As discussed in Section 4, although the closed dislocation loop C always induces a unique elastic field, the open dislocation segment AB taken out of this loop yields non-unique solutions (see, e.g., Hirth and Lothe, 1982; Wang, 1996). Due to the above fact, we stipulate that the displacement and stress fields of the dislocation segment AB share the same form with those of the dislocation loop C, as given in Eqs. (28a)–(29c). However, the involved integrals originally defined in Eqs. (30) and (32) have to be integrated along the straight segment AB, rather than the closed loop C.

From the original integrals on C in Eqs. (30) and (32), we can also obtain the corresponding integrals on AB as

$$\vec{\Phi}(\mathbf{x}) = \mathrm{sgn}\langle S(x_1, x_2) - x_3\rangle\left[\arctan\frac{(x_{2B} - x_{2A})t - (x_2 - x_{2A})}{(x_{1B} - x_{1A})t - (x_1 - x_{1A})}\right]\Bigg|_0^1 \tag{39}$$

where $S(x_1, x_2)$ is defined the same as that in Eq. (30), and

$$\overbrace{\vec{\mathrm{I}}^{\cdots}_{N;mk}}^{M}(\mathbf{x}) = \begin{cases} \frac{(x_{kB} - x_{kA})}{l^N_{\mathrm{pn}}}\int_0^1 \frac{\overbrace{[(x_{iB} - x_{iA})t - (x_i - x_{iA})]\cdots}^{M}}{\Upsilon^N_{\mathrm{pn}}R_m}dt \ \text{for}\ l_{\mathrm{pn}} \neq 0 \\ \frac{(x_{kB} - x_{kA})}{d^N_{\mathrm{pn}}}\int_0^1 \frac{\overbrace{[(x_{iB} - x_{iA})t - (x_i - x_{iA})]\cdots}^{M}}{R_m}dt \ \text{for}\ l_{\mathrm{pn}} = 0,\ d_{\mathrm{pn}} \neq 0 \end{cases}$$

$$\overbrace{\vec{\mathrm{J}}^{\cdots}_{N;mk}}^{M}(\mathbf{x}) = \begin{cases} \frac{(x_{kB} - x_{kA})}{l^N_{\mathrm{pn}}}\int_0^1 \frac{\overbrace{[(x_{iB} - x_{iA})t - (x_i - x_{iA})]\cdots}^{M}}{\Upsilon^N_{\mathrm{pn}}R^3_m}dt \ \text{for}\ l_{\mathrm{pn}} \neq 0 \\ \frac{(x_{kB} - x_{kA})}{d^N_{\mathrm{pn}}}\int_0^1 \frac{\overbrace{[(x_{iB} - x_{iA})t - (x_i - x_{iA})]\cdots}^{M}}{R^3_m}dt \ \text{for}\ l_{\mathrm{pn}} = 0,\ d_{\mathrm{pn}} \neq 0 \end{cases} \tag{40}$$

where the over-arrow "→" denotes a directional straight dislocation line, and

$$\Upsilon_{\mathrm{pn}}(t; x_\beta) = r_{\mathrm{pn}}[y_\alpha(t); x_\beta]/l_{\mathrm{pn}} = \sqrt{D^2_{\mathrm{pn}} - 2T_{\mathrm{pn}}t + t^2} \geqslant 0 \ \ (l_{\mathrm{pn}} \neq 0)$$
$$R_i(t; \mathbf{x}) = R_i[\mathbf{y}(t); \mathbf{x}] = \sqrt{l_i^2(D_i^2 - 2T_i t + t^2)} \tag{41}$$

in which

$$D_{\mathrm{pn}} = \frac{d_{\mathrm{pn}}}{l_{\mathrm{pn}}} \ \ (l_{\mathrm{pn}} \neq 0), \ \ T_{\mathrm{pn}} = \frac{\mathbf{d}_{\mathrm{pn}} \cdot \mathbf{l}_{\mathrm{pn}}}{l^2_{\mathrm{pn}}} \ \ (l_{\mathrm{pn}} \neq 0); \ \ D_i = \frac{d_i}{l_i}, \ \ T_i = \frac{\mathbf{d}_i \cdot \mathbf{l}_i}{l_i^2} \tag{42a}$$

and

$$\mathbf{l}_{\mathrm{pn}} = \{(x_{1B} - x_{1A}), (x_{2B} - x_{2A})\}, \quad l_{\mathrm{pn}} = \sqrt{(x_{1B} - x_{1A})^2 + (x_{2B} - x_{2A})^2};$$
$$\mathbf{l}_i = \{(x_{1B} - x_{1A}), (x_{2B} - x_{2A}), (x_{3B} - x_{3A})/\gamma_i\},$$
$$l_i = \sqrt{(x_{1B} - x_{1A})^2 + (x_{2B} - x_{2A})^2 + (x_{3B} - x_{3A})^2/\gamma_i^2};$$
$$\mathbf{d}_{\mathrm{pn}} = \{(x_1 - x_{1A}), (x_2 - x_{2A})\}, \quad d_{\mathrm{pn}} = \sqrt{(x_1 - x_{1A})^2 + (x_2 - x_{2A})^2};$$
$$\mathbf{d}_i = \{(x_1 - x_{1A}), (x_2 - x_{2A}), (x_3 - x_{3A})/\gamma_i\},$$
$$d_i = \sqrt{(x_1 - x_{1A})^2 + (x_2 - x_{2A})^2 + (x_3 - x_{3A})^2/\gamma_i^2} \tag{42b}$$

Note that l_i (or d_i) is the length of the vector $\mathbf{l}_i$ (or $\mathbf{d}_i$) and should not be confused with the ith component of this vector.

According to the properties of the integrals defined in Eq. (40), three orientation cases of AB are considered in detail as follows.

Case 1. A straight dislocation segment normal to the plane of isotropy ($l_{\mathrm{pn}} = 0$)

In this case, we assume that AB lies on the intersection of two planes $x_\alpha = x_{\alpha\mathrm{const}}$, where $x_{\alpha\mathrm{const}}$ are two constants. When $d_{\mathrm{pn}} \neq 0$, Eqs. (28a)–(29c) can be reduced to

$$u_\xi(\mathbf{x}) = \frac{b_3}{4\pi}(x_{\alpha\mathrm{const}} - x_\alpha)\frac{g_i}{\gamma_i}\varepsilon_{\alpha\xi 3}\vec{\mathrm{I}}^{3}_{2;i3} - \frac{b_\beta}{4\pi}\frac{1}{\gamma_3}\varepsilon_{\xi\beta 3}\vec{\tilde{\mathrm{I}}}_{0;33} - \frac{b_\beta}{4\pi}\frac{2}{\gamma_3^2}\gamma_i f_i \times\left[(x_{\xi\mathrm{const}} - x_\xi)(x_{\alpha\mathrm{const}} - x_\alpha)\varepsilon_{\alpha\beta 3}\left(2\vec{\mathrm{I}}^{33}_{4;i3}/\gamma_i^2 + \vec{\tilde{\mathrm{I}}}_{2;i3}\right) - \varepsilon_{\xi\beta 3}\left(\vec{\mathrm{I}}^{33}_{2;i3}/\gamma_i^2 + \vec{\tilde{\mathrm{I}}}_{0;i3}\right)\right] \tag{43a}$$

$$u_3(\mathbf{x}) = \frac{b_\beta}{4\pi}(x_{\alpha\mathrm{const}} - x_\alpha)\frac{2}{\gamma_3^2}\frac{m_\eta f_\eta}{\gamma_\eta}\varepsilon_{\alpha\beta 3}\vec{\mathrm{I}}^{3}_{2;\eta 3} \tag{43b}$$

and

$$\sigma_{\xi\eta}(\mathbf{x}) = \delta_{\xi\eta}\frac{c_{44}b_\beta}{4\pi}\frac{2}{\gamma_3^2}(x_{\alpha\text{const}}-x_\alpha)\varepsilon_{\alpha\beta3}\left[\left(\frac{g_i}{\gamma_i}-\frac{2}{\gamma_3^2}\gamma_i f_i\right)\tilde{\vec{J}}_{0;i3}+\frac{2}{\gamma_3^2}\gamma_i f_i\left(\tilde{\vec{I}}_{2;i3}+\frac{2}{\gamma_i^2}\vec{I}^{33}_{4;i3}\right)\right]$$
$$+\frac{c_{44}}{4\pi}\frac{2}{\gamma_3^2}\left\{\begin{array}{l} b_\beta\frac{2}{\gamma_3^2}\gamma_i f_i\left[\begin{array}{l}(x_{\alpha\text{const}}-x_\alpha)(x_{\xi\text{const}}-x_\xi)(x_{\eta\text{const}}-x_\eta)\varepsilon_{\alpha\beta3}(\tilde{\vec{J}}_{2;i3}-4\tilde{\vec{I}}_{4;i3}-\frac{8}{\gamma_i^2}\vec{I}^{33}_{6;i3})\\ +[(x_{\xi\text{const}}-x_\xi)\varepsilon_{\eta\beta3}+(x_{\eta\text{const}}-x_\eta)\varepsilon_{\xi\beta3}](\tilde{\vec{I}}_{2;i3}+2\vec{I}^{33}_{4;i3}/\gamma_i^2)\end{array}\right]\\ +\frac{1}{2}b_3\frac{g_i}{\gamma_i}(x_{\alpha\text{const}}-x_\alpha)[(x_{\xi\text{const}}-x_\xi)\varepsilon_{\alpha\eta3}+(x_{\eta\text{const}}-x_\eta)\varepsilon_{\alpha\xi3}](\tilde{\vec{J}}^3_{2;i3}+2\vec{I}^3_{4;i3})\end{array}\right\} \tag{44a}$$

$$\sigma_{\xi3}(\mathbf{x}) = -\frac{c_{44}b_3}{4\pi}(x_{\alpha\text{const}}-x_\alpha)\frac{h_i}{\gamma_i}\varepsilon_{\alpha\xi3}\tilde{\vec{J}}_{0;i3}-\frac{c_{44}b_\beta}{4\pi}$$
$$\times\left\{\frac{2}{\gamma_3^2}\frac{g_i}{\gamma_i}\left[\varepsilon_{\xi\beta3}\vec{I}^3_{2;i3}-(x_{\xi\text{const}}-x_\xi)(x_{\alpha\text{const}}-x_\alpha)\varepsilon_{\alpha\beta3}\right.\right.$$
$$\left.\left.\times\left(\tilde{\vec{J}}^3_{2;i3}+2\vec{I}^3_{4;i3}\right)\right]+\frac{1}{\gamma_3^2}\varepsilon_{\xi\beta3}\tilde{\vec{J}}^3_{0;33}\right\} \tag{44b}$$

$$\sigma_{33}(\mathbf{x}) = -\frac{c_{44}b_\beta}{4\pi}\frac{2}{\gamma_3^2}(x_{\alpha\text{const}}-x_\alpha)\gamma_\eta g_\eta\varepsilon_{\alpha\beta3}\tilde{\vec{J}}_{0;\eta3} \tag{44c}$$

The involved functions $\vec{I}$ and $\vec{J}$ in Eqs. (43a)–(44c) can be reduced to two types of integrals below (Gradshteyn and Ryzhik, 2007)

$$\text{Int.} = \int_0^1 \frac{P_n(t)}{R_m(t;\mathbf{x})}\mathrm{d}t\ \ (n=0,1,2);\quad \text{Int.} = \int_0^1 \frac{P_n(t)}{R_m^3(t;\mathbf{x})}\mathrm{d}t\ \ (n=0,1) \tag{45}$$

where $P_n(t)$ is a polynomial of degree n with respect to t.

Eq. (45) can be further expressed in terms of two basic integrals below

$$\int_0^1 \frac{\mathrm{d}t}{R_m(t;\mathbf{x})} = \frac{1}{l_m}\{\ln[R_m+l_m(t-T_m)]\}\Big|_0^1;$$
$$\int_0^1 \frac{\mathrm{d}t}{R_m^3(t;\mathbf{x})} = \frac{1}{l_m^2(D_m^2-T_m^2)}\left(\frac{t-T_m}{R_m}\right)\Big|_0^1 \tag{46}$$

where the trivial case of $D_m{}^2 = T_m{}^2$ (i.e., $\mathbf{d}_m\times\mathbf{l}_m = 0$) is omitted due to its simplicity. Analytical expressions of the line integrals needed in Eqs. (43a)–(44c) for Case 1 are given in Appendix A.

Alternatively, by introducing three higher-order potential functions ψ_i defined as

$$\chi_i(\mathbf{y};\mathbf{x}) = \gamma_i\frac{\partial\psi_i(\mathbf{y};\mathbf{x})}{\partial y_3};$$
$$\psi_i(\mathbf{y};\mathbf{x}) = \left\{\begin{array}{l} -\left[\frac{3}{4}\frac{(y_3-x_3)^2}{\gamma_i^2}-\frac{1}{4}R_i^2\right]\ln(R_i-\frac{y_3-x_3}{\gamma_i})-\frac{3}{4}\frac{y_3-x_3}{\gamma_i}R_i\\ \quad\text{for } x_3 > S(x_1,x_2)\ \text{ with }\ C_{\text{pn}}(x_1,x_2)\leqslant 0.\\ +\left[\frac{3}{4}\frac{(y_3-x_3)^2}{\gamma_i^2}-\frac{1}{4}R_i^2\right]\ln(R_i+\frac{y_3-x_3}{\gamma_i})-\frac{3}{4}\frac{y_3-x_3}{\gamma_i}R_i\\ \quad\text{for } x_3 < S(x_1,x_2)\ \text{ with }\ C_{\text{pn}}(x_1,x_2)\leqslant 0;\ \text{ or }\ C_{\text{pn}}(x_1,x_2)>0.\end{array}\right. \tag{47}$$

the elastic field solution in Eqs. (43a)–(44c) can then be rewritten concisely as

$$u_i(\mathbf{x}) = \tilde{u}_i(x_{1\text{const}},x_{2\text{const}},x_{3B};\mathbf{x})-\tilde{u}_i(x_{1\text{const}},x_{2\text{const}},x_{3A};\mathbf{x})$$
$$\sigma_{ij}(\mathbf{x}) = \tilde{\sigma}_{ij}(x_{1\text{const}},x_{2\text{const}},x_{3B};\mathbf{x})-\tilde{\sigma}_{ij}(x_{1\text{const}},x_{2\text{const}},x_{3A};\mathbf{x}) \tag{48}$$

where

$$\tilde{u}_3(\mathbf{y};\mathbf{x}) = -\frac{b_\beta}{4\pi}\varepsilon_{\alpha\beta3}\frac{2}{\gamma_3^2}\frac{\partial(f_\eta m_\eta\gamma_\eta\chi_\eta)}{\partial y_\alpha}$$
$$\tilde{u}_\xi(\mathbf{y};\mathbf{x}) = -\frac{b_\beta}{4\pi}\left[\varepsilon_{\xi\beta3}\frac{\partial(\gamma_3\chi_3)}{\partial y_3}+\varepsilon_{\alpha\beta3}\frac{2}{\gamma_3^2}\frac{\partial^2(f_i\gamma_i^2\psi_i)}{\partial y_\xi\partial y_\alpha}\right]-\frac{b_3}{4\pi}\varepsilon_{\alpha\xi3}\frac{\partial(g_i\gamma_i\chi_i)}{\partial y_\alpha}$$
$$\tilde{\sigma}_{33}(\mathbf{y};\mathbf{x}) = \frac{c_{44}b_\beta}{4\pi}\varepsilon_{\alpha\beta3}\frac{2}{\gamma_3^2}\frac{\partial^2(g_\eta\gamma_\eta^3\chi_\eta)}{\partial y_\alpha\partial y_3}$$
$$\tilde{\sigma}_{\xi3}(\mathbf{y};\mathbf{x}) = \frac{c_{44}b_\beta}{4\pi}\left[\varepsilon_{\alpha\beta3}\frac{2}{\gamma_3^2}\frac{\partial^2(g_i\gamma_i\chi_i)}{\partial y_\alpha\partial y_\xi}+\varepsilon_{\xi\beta3}\frac{\partial^2(\gamma_3\chi_3)}{\partial y_3^2}\right]+\frac{c_{44}b_3}{4\pi}\varepsilon_{\alpha\xi3}\frac{\partial^2(h_i\gamma_i\chi_i)}{\partial y_\alpha\partial y_3}$$
$$\tilde{\sigma}_{\xi\eta}(\mathbf{y};\mathbf{x}) = \frac{c_{44}b_\beta}{4\pi}\varepsilon_{\alpha\beta3}\frac{2}{\gamma_3^2}\left[\delta_{\xi\eta}\frac{\partial^2}{\partial y_\alpha\partial y_3}\left(\frac{2}{\gamma_3^2}f_i\gamma_i^3\chi_i-g_i\gamma_i\chi_i\right)+\frac{2}{\gamma_3^2}\frac{\partial^3(f_i\gamma_i^2\psi_i)}{\partial y_\alpha\partial y_\xi\partial y_\eta}\right]$$
$$+\frac{c_{44}b_3}{4\pi}\frac{1}{\gamma_3^2}\left(\varepsilon_{\alpha\xi3}\frac{\partial}{\partial y_\eta}+\varepsilon_{\alpha\eta3}\frac{\partial}{\partial y_\xi}\right)\frac{\partial(g_i\gamma_i\chi_i)}{\partial y_\alpha} \tag{49}$$

Note that the elastic field solution given in Eq. (48) is also applicable to the trivial case of $d_{\text{pn}} = 0$.

Case 2. A straight dislocation segment parallel to the plane of isotropy ($T_m \equiv T_{\text{pn}}$)

In this case, we assume that AB lies on the plane $x_3 = x_{3\text{const}}$, where $x_{3\text{const}}$ is a constant. Thus the elastic field solutions have the same form as in Eqs. (35a)–(36c). The involved functions $\vec{I}$ and $\vec{J}$ can be reduced to the following integrals

$$\text{Int.} = \int_{\tau_0}^{\tau_1}\frac{P_n(\tau)\mathrm{d}\tau}{(\lambda_{\text{pn}}+\tau^2)^{N/2}[l_m^2(\lambda_m+\tau^2)]^{Z/2}}$$
$$\left(\begin{array}{l} Z=1;\ N=0,2,4;\ n=0,1,2;\ n\leqslant N\\ \text{or } Z=3;\ N=0,2;\ n=0,1,2;\ n\leqslant N+1\end{array}\right) \tag{50}$$

with

$$\tau_0 = -T_{\text{pn}},\quad \tau_1 = 1-T_{\text{pn}};$$
$$\lambda_{\text{pn}} = D_{\text{pn}}^2-T_{\text{pn}}^2\geqslant 0,\quad \lambda_m = D_m^2-T_{\text{pn}}^2 \tag{51}$$

where $\lambda_m = \lambda_{\text{pn}}$ if and only if $x_3 = x_{3\text{const}}$, and $\lambda_{\text{pn}} = 0$ if and only if $(\mathbf{d}_m\times\mathbf{l}_m)\cdot\mathbf{k} = 0$, with $\mathbf{k}$ being the unit basis vector in the x_3-direction of the Cartesian coordinates.

Eq. (50) can be further expressed as a linear combination of two types of integrals below (Gradshteyn and Ryzhik, 2007)

$$\text{Int.} = \int_{\tau_0}^{\tau_1}\frac{\tau\mathrm{d}\tau}{(\lambda_{\text{pn}}+\tau^2)^{N_1/2}[l_m^2(\lambda_m+\tau^2)]^{Z/2}}$$
$$= \frac{\sqrt{l_m^2(\lambda_m-\lambda_{\text{pn}})}}{l_m^{(Z+1)}(\lambda_m-\lambda_{\text{pn}})^{(N_1+Z-1)/2}}\times\int_{\xi(\tau_0)}^{\xi(\tau_1)}\frac{\mathrm{d}\xi}{(\xi^2-1)^{N_1/2}\xi^{Z-1}}\quad(\lambda_m\neq\lambda_{pn};N_1\text{ is even},Z=1,3) \tag{52a}$$

$$\text{Int.} = \int_{\tau_0}^{\tau_1}\frac{\mathrm{d}\tau}{(\lambda_{\text{pn}}+\tau^2)^{N_2/2}[l_m^2(\lambda_m+\tau^2)]^{Z/2}}$$
$$= \int_{\zeta(\tau_0)}^{\zeta(\tau_1)}\frac{[1-\lambda_{\text{pn}}\zeta^2/(\lambda_m-\lambda_{\text{pn}})]^{(N_2+Z-3)/2}\mathrm{d}\zeta}{\sqrt{l_m^2(\lambda_m-\lambda_{\text{pn}})}l_m^{(Z-1)}\lambda_m^{(Z-1)/2}\lambda_{\text{pn}}^{(N_2-1)/2}(\zeta^2+1)^{N_2/2}}$$
$$(\lambda_m\neq\lambda_{pn},\lambda_{pn}\neq0;N_2\text{ is even},Z=1,3) \tag{52b}$$

with

$$\xi(\tau)=\frac{\sqrt{l_m^2(\lambda_m+\tau^2)}}{\sqrt{l_m^2(\lambda_m-\lambda_{\rm pn})}}\quad(\lambda_m\neq\lambda_{\rm pn});$$
$$\zeta(\tau)=\frac{\sqrt{l_m^2(\lambda_m-\lambda_{\rm pn})}}{\sqrt{\lambda_{\rm pn}}}\frac{\tau}{\sqrt{l_m^2(\lambda_m+\tau^2)}}\quad(\lambda_m\neq\lambda_{\rm pn},\ \ \lambda_{\rm pn}\neq 0) \tag{53}$$

The trivial case of $\lambda_m=\lambda_{\rm pn}$ or $\lambda_{\rm pn}=0$ is omitted here due to its simplicity.

It can be shown that, Eqs. (52a,b) can be integrated analytically in terms of elementary functions via the following recurrence relations

$$\int\frac{{\rm d}z}{(z^2-1)^n z^2}=-\int\frac{1}{(z^2-1)^{n-1}z^2}{\rm d}z+\int\frac{{\rm d}z}{(z^2-1)^n}\quad(n\in\mathbb{N});$$
$$\int\frac{(1-az^2)^{n_1}}{(z^2+1)^{n_2}}{\rm d}z=(1+a)\int\frac{(1-az^2)^{n_1-1}}{(z^2+1)^{n_2}}{\rm d}z-a\int\frac{(1-az^2)^{n_1-1}}{(z^2+1)^{n_2-1}}{\rm d}z\quad(n_1,n_2\in\mathbb{N});$$
$$\int\frac{{\rm d}z}{(z^2\pm1)^{n+1}}=\pm\frac{2n-1}{2n}\int\frac{{\rm d}z}{(z^2\pm1)^n}\pm\frac{1}{2n}\frac{z}{(z^2\pm1)^n}\quad(n\in\mathbb{N});$$
$$\int\frac{{\rm d}z}{z^2-1}=\frac{1}{2}\ln\frac{z-1}{z+1};\quad\int\frac{{\rm d}z}{z^2+1}=\arctan z=\frac{1}{2{\rm i}}\ln\frac{z-{\rm i}}{z+{\rm i}}\ \text{ with }\ {\rm i}=\sqrt{-1} \tag{54}$$

Analytical expressions of the line integrals needed in Eqs. (35a)–(36c) for Case 2 are given in Appendix B.

Case 3. A straight dislocation segment neither normal nor parallel to the plane of isotropy ($l_{\rm pn}\neq 0$ and $T_m\not\equiv T_{\rm pn}$).

In this case, the integrals defined in Eq. (40) can always be expressed in terms of linear combinations of the integrals in Eq. (45) and those of the form

$$\text{Int.}=\int_0^1\frac{\alpha t+\beta}{\Upsilon_{\rm pn}^N R_m^Z}dt\ \ (N=2,4,6;\ \ Z=1,3;\ \ \alpha,\beta\ \text{ are constants}) \tag{55}$$

where $\gamma_{\rm pn}$ and R_m are defined the same as those in Eq. (41).

It can be shown that $T_m=T_{\rm pn}$ if and only if $[\mathbf{l}_m\times(\mathbf{d}_m\times\mathbf{l}_m)]\cdot\mathbf{k}=0$, with $\mathbf{k}$ being again the unit basis vector in the x_3-direction of the Cartesian coordinates. For the trivial case of $T_m=T_{\rm pn}$, one only needs to follow the same procedure as presented for Case 2. We thus discuss the non-trivial case in which $T_m\neq T_{\rm pn}$.

By means of the following substitution (Gradshteyn and Ryzhik, 2007, where a printing error has been corrected here)

$$t=\varpi_1+\varpi_2\frac{\tau-1}{\tau+1} \tag{56}$$

with

$$\varpi_1=\frac{1}{2}\frac{D_m^2-D_{\rm pn}^2}{T_m-T_{\rm pn}};$$
$$\varpi_2=\frac{1}{2}\frac{\sqrt{(D_m^2-D_{\rm pn}^2)^2-4(D_m^2T_{\rm pn}-D_{\rm pn}^2T_m)(T_m-T_{\rm pn})}}{T_m-T_{\rm pn}} \tag{57}$$

the integrals in Eq. (55) can be transformed into those of the form

$$\text{Int.}=\int\frac{{\rm sgn}\langle\tau+1\rangle P_n(\tau){\rm d}\tau}{(\lambda_{\rm pn}+\tau^2)^{N/2}[(l_m^2\lambda_m^+)(\lambda_m+\tau^2)]^{Z/2}}\quad\begin{pmatrix}N=2,4,6;\ \ Z=1,3;\\ 0\leq n\leq N+Z-2,\ \ n+1\in\mathbb{N}\end{pmatrix} \tag{58}$$

with

$$\lambda_{\rm pn}=\frac{\lambda_{\rm pn}^-}{\lambda_{\rm pn}^+}\geqslant 0,\ \ \lambda_m=\frac{\lambda_m^-}{\lambda_m^+}\neq 0;\quad l_m^2\lambda_m^+=l_{\rm pn}^2\lambda_{\rm pn}^+>0 \tag{59}$$

where

$$\lambda_{\rm pn}^+=D_{\rm pn}^2-2T_{\rm pn}(\varpi_1+\varpi_2)+(\varpi_1+\varpi_2)^2>0$$
$$\lambda_{\rm pn}^-=D_{\rm pn}^2-2T_{\rm pn}(\varpi_1-\varpi_2)+(\varpi_1-\varpi_2)^2\geqslant 0$$
$$\lambda_m^+=D_m^2-2T_m(\varpi_1+\varpi_2)+(\varpi_1+\varpi_2)^2\neq 0$$
$$\lambda_m^-=D_m^2-2T_m(\varpi_1-\varpi_2)+(\varpi_1-\varpi_2)^2\neq 0 \tag{60}$$

in which $\lambda_{\rm pn}^-=0$ if and only if $(\mathbf{d}_m\times\mathbf{l}_m)\cdot\mathbf{k}=0$.

When handling the integrals in Eq. (58), one should keep in mind the following two important points:

(i) Regardless of the complexity of γ_α, the integral variable τ is always real-valued due to the following relations

$$\varpi_1\in\mathbb{R};\quad\varpi_1-\varpi_2=\frac{M_{i3}}{W_{i3}}\in\mathbb{R};$$
$$\frac{(D_i^2-D_{\rm pn}^2)^2-4(D_i^2T_{\rm pn}-D_{\rm pn}^2T_i)(T_i-T_{\rm pn})}{(T_i-T_{\rm pn})^2}=\frac{(V_{i1}^2+V_{i2}^2)^2}{\left[W_{i3}(x'_{3B}-x'_{3A})/\gamma_i\right]^2}>0 \tag{61}$$

where

$$\mathbf{d}_i\times\mathbf{l}_i=\{V_{i1},V_{i2},V_{i3}\}$$
$$\mathbf{l}_i\times(\mathbf{d}_i\times\mathbf{l}_i)=\{W_{i1},W_{i2},W_{i3}\}$$
$$\mathbf{d}_i\times(\mathbf{d}_i\times\mathbf{l}_i)=\{M_{i1},M_{i2},M_{i3}\} \tag{62}$$

(ii) When $\min\{x_{3A},x_{3B}\}<x_3<\max\{x_{3A},x_{3B}\}$, the integral interval with respect to τ must be divided into two parts because of the following relation

$$\varpi_1+\varpi_2=\frac{x_3-x_{3A}}{x_{3B}-x_{3A}}\in(0,1)$$
$$\text{when}\ \ \min\{x_{3A},x_{3B}\}<x_3<\max\{x_{3A},x_{3B}\} \tag{63}$$

Based on the above observations, the integral in Eq. (58) is equivalent to

$$\begin{aligned}\text{Int.}&=\text{sgn}\langle\tau_0+1\rangle\int_{\tau_0}^{\infty{\rm sgn}\langle\tau_0+1\rangle}\frac{P_n(\tau){\rm d}\tau}{(\lambda_{\rm pn}+\tau^2)^{N/2}[(l_m^2\lambda_m^+)(\lambda_m+\tau^2)]^{Z/2}}\\&+\text{sgn}\langle\tau_1+1\rangle\int_{\infty{\rm sgn}\langle\tau_1+1\rangle}^{\tau_1}\frac{P_n(\tau){\rm d}\tau}{(\lambda_{\rm pn}+\tau^2)^{N/2}[(l_m^2\lambda_m^+)(\lambda_m+\tau^2)]^{Z/2}}\end{aligned} \tag{64}$$

in which

$$\tau_0=\frac{\varpi_2-\varpi_1}{\varpi_2+\varpi_1},\quad\tau_1=\frac{\varpi_2-(\varpi_1-1)}{\varpi_2+(\varpi_1-1)}. \tag{65}$$

For further reduction and simplification of Eq. (64), we only need to follow exactly the same procedure as presented in Case 2. Analytical expressions of the line integrals needed in Eqs. (28a)–(29c) for Case 3 are listed in Appendix C.

As an immediate application of the above analytical integrals, we now calculate the quasi solid angle Ω_3 of an arbitrary polygonal dislocation loop $ABC\ldots DA$, which consists of a finite number of straight dislocation segments $AB, BC, \ldots$ and DA. By virtue of Eq. (33), we are able to derive an explicit formula for Ω_3 as

$$\Omega_3(\mathbf{x})=-\Phi-\frac{1}{\gamma_3}\left[(\text{I}_{2;31}^{23}-\text{I}_{2;32}^{13})_{AB}+(\text{I}_{2;31}^{23}-\text{I}_{2;32}^{13})_{BC}\cdots+(\text{I}_{2;31}^{23}-\text{I}_{2;32}^{13})_{DA}\right] \tag{66}$$

where, for example,

$$\begin{aligned}(\text{I}_{2;31}^{23}-\text{I}_{2;32}^{13})_{AB}=&\frac{4\varpi_2^2(x_{3B}-x_{3A})[(x_{1B}-x_{1A})(x_2-x_{2A})-(x_1-x_{1A})(x_{2B}-x_{2A})]}{l_{\rm pn}^3(\lambda_{\rm pn}^+)^{3/2}\sqrt{\lambda_{\rm pn}}\sqrt{\lambda_3-\lambda_{\rm pn}}}\\&\times[\text{sgn}\langle\tau_0+1\rangle\arctan\zeta(\tau)|_{\tau_0}^{\infty{\rm sgn}\langle\tau_0+1\rangle}\\&+\text{sgn}\langle\tau_1+1\rangle\arctan\zeta(\tau)|_{\infty{\rm sgn}\langle\tau_1+1\rangle}^{\tau_1}]\end{aligned} \tag{67a}$$

corresponding to Case 3,

$$\begin{aligned}(\text{I}_{2;31}^{23}-\text{I}_{2;32}^{13})_{AB}=&\frac{(x_3-x_{3A})[(x_{1B}-x_{1A})(x_2-x_{2A})-(x_1-x_{1A})(x_{2B}-x_{2A})]}{l_{\rm pn}^2l_3\sqrt{\lambda_{\rm pn}}\sqrt{\lambda_3-\lambda_{\rm pn}}}\\&\times\arctan\zeta(\tau)|_{\tau_0}^{\tau_1}\end{aligned} \tag{67b}$$

corresponding to Case 2, and

$$(\text{I}_{2;31}^{23}-\text{I}_{2;32}^{13})_{AB}=0 \tag{67c}$$

corresponding to Case 1, and the calculation of Φ has been illustrated in Section 5.

The most striking advantage of Eqs. (67a–c) lies in the fact that, the result is totally determined by two end points $A(x_{1A}, x_{2A}, x_{3A})$ and $B(x_{1B}, x_{2B}, x_{3B})$ of the straight segment AB and one field point (x_1, x_2, x_3); thus one does not need to introduce any auxiliary point into the calculation and know any information about the cut surface. Moreover, the function $\arctan(x)$ is single-valued which ranges from $-\pi/2$ to $\pi/2$. In other words, Eqs. (67a–c) is very convenient and efficient in calculating the quasi solid angle Ω_3 and the traditional solid angle Ω ($\gamma_3 = 1$ in this case). The related issue was also discussed by Barnett (1985, 2007).

In summary, for a straight dislocation segment of arbitrary orientation, the induced displacement and stress fields are expressed in terms of elementary functions. We also remark that our stress formulae for segments are more explicit than Willis' formula (Willis, 1970) in the transversely isotropic case, and that, to the best of our knowledge, the displacement formulae for segments presented in this paper are new and simple. In the next section, we return to the closed dislocation loop case and provide a new analytical solution for a circular dislocation loop parallel to the plane of isotropy.

7. A circular dislocation loop parallel to the plane of isotropy

As a special case of our solutions (35a)–(36c) in Section 5, we now consider a flat, circular dislocation loop of radius r_0 parallel to the plane of isotropy with its center at the origin of coordinates. The Burgers vector $\boldsymbol{b}$ (b_1, b_2, b_3) over the circle is uniform and the induced fields are expressed in terms of the cylindrical coordinates (ρ, θ, x_3).

From Eqs. (35a)–(36c), the displacements and stresses can be written explicitly as

$$\begin{aligned} u_1 &= -\tfrac{1}{4\pi}\{b_1\Omega_3 + 2r_0 b_3\cos\theta(\gamma_\alpha g_\alpha I_{1\alpha}) \\ &\quad + r_0 x_3 \tfrac{g_i}{\gamma_i}[b_1 I_{2i} + (b_1\cos 2\theta + b_2\sin 2\theta)I_{3i}]\} \\ u_2 &= -\tfrac{1}{4\pi}\{b_2\Omega_3 + 2r_0 b_3\sin\theta(\gamma_\alpha g_\alpha I_{1\alpha}) \\ &\quad + r_0 x_3 \tfrac{g_i}{\gamma_i}[b_2 I_{2i} + (b_1\sin 2\theta - b_2\cos 2\theta)I_{3i}]\} \end{aligned} \tag{68a}$$

$$u_3 = -\frac{1}{4\pi}\left[b_3 m_\alpha g_\alpha \Omega_\alpha + 2r_0(b_1\cos\theta + b_2\sin\theta)\frac{m_\alpha g_\alpha}{\gamma_\alpha} I_{1\alpha}\right] \tag{68b}$$

and

$$\begin{aligned} \sigma_{11} &= \tfrac{c_{44}r_0}{2\pi} x_3\left(b_1\cos\theta + b_2\sin\theta\right)\left[\left(\tfrac{2}{\gamma_3^2}\tfrac{g_\alpha}{\gamma_\alpha} - \tfrac{h_\alpha}{\gamma_\alpha^3}\right)J_{1\alpha} - \tfrac{2}{\gamma_3^2}\tfrac{g_i}{\gamma_i}(\cos^2\theta\tfrac{I_{4i}}{\rho} + \sin^2\theta\tfrac{I_{3i}}{\rho})\right] \\ &\quad + \tfrac{c_{44}r_0}{\pi} x_3 b_1\cos\theta\left(\tfrac{1}{\gamma_3^3}J_{13} - \tfrac{2}{\gamma_3^2}\tfrac{g_i}{\gamma_i}\tfrac{I_{3i}}{\rho}\right) + \tfrac{c_{44}r_0}{2\pi} b_3\left[\left(\tfrac{\gamma_\alpha g_\alpha}{\gamma_3^2} - \tfrac{h_\alpha}{\gamma_\alpha}\right)J_{2\alpha} - \cos 2\theta(\tfrac{\gamma_\alpha g_\alpha}{\gamma_3^2}J_{3\alpha})\right] \end{aligned}$$

$$\begin{aligned} \sigma_{22} &= \tfrac{c_{44}r_0}{2\pi} x_3\left(b_1\cos\theta + b_2\sin\theta\right)[(\tfrac{2}{\gamma_3^2}\tfrac{g_\alpha}{\gamma_\alpha} - \tfrac{h_\alpha}{\gamma_\alpha^3})J_{1\alpha} - \tfrac{2}{\gamma_3^2}\tfrac{g_i}{\gamma_i}(\sin^2\theta\tfrac{I_{4i}}{\rho} + \cos^2\theta\tfrac{I_{3i}}{\rho})] \\ &\quad + \tfrac{c_{44}r_0}{\pi} x_3 b_2\sin\theta(\tfrac{1}{\gamma_3^3}J_{13} - \tfrac{2}{\gamma_3^2}\tfrac{g_i}{\gamma_i}\tfrac{I_{3i}}{\rho}) + \tfrac{c_{44}r_0}{2\pi} b_3[(\tfrac{\gamma_\alpha g_\alpha}{\gamma_3^2} - \tfrac{h_\alpha}{\gamma_\alpha})J_{2\alpha} + \cos 2\theta(\tfrac{\gamma_\alpha g_\alpha}{\gamma_3^2}J_{3\alpha})] \end{aligned}$$

$$\begin{aligned} \sigma_{12} &= -\frac{c_{44}r_0}{2\pi} b_3\sin 2\theta\left(\frac{\gamma_\alpha g_\alpha}{\gamma_3^2}J_{3\alpha}\right) + \frac{c_{44}r_0}{2\pi} x_3(b_1\sin\theta + b_2\cos\theta)\frac{1}{\gamma_3^3}J_{13} \\ &\quad - \frac{c_{44}r_0}{2\pi} x_3\frac{2}{\gamma_3^2}\frac{g_i}{\gamma_i}\left[b_1\sin\theta\left(\cos^2\theta\frac{J_{4i}}{\rho} + \sin^2\theta\frac{I_{3i}}{\rho}\right)\right. \\ &\quad \left. + b_2\cos\theta\left(\sin^2\theta\frac{J_{4i}}{\rho} + \cos^2\theta\frac{I_{3i}}{\rho}\right)\right] \end{aligned} \tag{69a}$$

$$\begin{aligned} \sigma_{13} &= \frac{c_{44}r_0}{4\pi}\left[b_1\left(\frac{1}{\gamma_3}J_{23} - \frac{h_\alpha}{\gamma_\alpha}J_{2\alpha}\right) - (b_1\cos 2\theta + b_2\sin 2\theta)\frac{h_i}{\gamma_i}J_{3i}\right. \\ &\quad \left. + 2x_3 b_3\cos\theta\left(\frac{h_\alpha}{\gamma_\alpha}J_{1\alpha}\right)\right] \end{aligned}$$

$$\begin{aligned} \sigma_{23} &= \frac{c_{44}r_0}{4\pi}\left[b_2\left(\frac{1}{\gamma_3}J_{23} - \frac{h_\alpha}{\gamma_\alpha}J_{2\alpha}\right) - (b_1\sin 2\theta - b_2\cos 2\theta)\frac{h_i}{\gamma_i}J_{3i}\right. \\ &\quad \left. + 2x_3 b_3\sin\theta\left(\frac{h_\alpha}{\gamma_\alpha}J_{1\alpha}\right)\right] \end{aligned} \tag{69b}$$

$$\sigma_{33} = \frac{c_{44}r_0}{2\pi}\left[x_3(b_1\cos\theta + b_2\sin\theta)\frac{h_\alpha}{\gamma_\alpha}J_{1\alpha} + b_3(\gamma_\alpha h_\alpha J_{2\alpha})\right] \tag{69c}$$

where (Gradshteyn and Ryzhik, 2007)

$$\Omega_i = \pi\,\mathrm{sgn}\langle x_3\rangle(1 + \mathrm{sgn}\langle r_0 - \rho\rangle) - 2r_0 x_3 I_{2i}/\gamma_i \tag{70}$$

and

$$\begin{aligned} I_{1\alpha} &= \int_0^\pi \frac{\cos\varphi\,\mathrm{d}\varphi}{R_\alpha} \\ &= \frac{\sqrt{p_\alpha + q}}{\rho r_0}\left[\frac{p_\alpha}{p_\alpha + q}K(k_\alpha) - E(k_\alpha)\right] \quad \text{for } \rho \neq 0 \end{aligned} \tag{71a}$$

$$\begin{aligned} I_{2i} &= \int_0^\pi \frac{r_0 - \rho\cos\varphi}{r_{\mathrm{pn}}^2 R_i}\mathrm{d}\varphi \\ &= \frac{1}{r_0\sqrt{p_i + q}}\left[K(k_i) + \frac{r_0 - \rho}{r_0 + \rho}\Pi(n, k_i)\right] \quad \text{for } \rho \neq r_0 \end{aligned} \tag{71b}$$

$$\begin{aligned} I_{3i} &= \int_0^\pi \frac{r_0\cos 2\varphi - \rho\cos\varphi}{r_{\mathrm{pn}}^2 R_i}\mathrm{d}\varphi \\ &= \frac{1}{r_0\sqrt{p_i + q}}\left[\frac{p_i + q}{\rho^2}E(k_i) - \frac{p_i + r_0^2}{\rho^2}K(k_i) + \frac{(r_0 - \rho)r_0^2}{(r_0 + \rho)\rho^2}\Pi(n, k_i)\right] \\ &\quad \text{for } \rho \neq r_0 \text{ and } \rho \neq 0 \end{aligned} \tag{71c}$$

and

$$J_{1i} = \int_0^\pi \frac{\cos\varphi\,\mathrm{d}\varphi}{R_i^3} = \frac{1}{\rho r_0\sqrt{p_i + q}}\left[\frac{p_i}{p_i - q}E(k_i) - K(k_i)\right] \quad \text{for } \rho \neq 0 \tag{72a}$$

$$J_{2i} = \int_0^\pi \frac{r_0 - \rho\cos\varphi}{R_i^3}\mathrm{d}\varphi = \frac{1}{r_0\sqrt{p_i + q}}\left[\frac{2r_0^2 - p_i}{p_i - q}E(k_i) + K(k_i)\right] \tag{72b}$$

$$\begin{aligned} J_{3i} &= \int_0^\pi \frac{r_0\cos 2\varphi - \rho\cos\varphi}{R_i^3}\mathrm{d}\varphi \\ &= \frac{1}{r_0\sqrt{p_i + q}}\left[\frac{p_i(2p_i - \rho^2) - 6\rho^2 r_0^2}{\rho^2(p_i - q)}E(k_i) - \frac{2p_i - \rho^2}{\rho^2}K(k_i)\right] \quad \text{for } \rho \neq 0 \end{aligned} \tag{72c}$$

$$J_{4i} = \rho\frac{\partial I_{3i}}{\partial\rho} - I_{3i} = \frac{1}{r_0\sqrt{p_i + q}}\begin{bmatrix} \frac{3q^2 - p_i(3p_i - \rho^2)}{(p_i - q)\rho^2}E(k_i) + \frac{3r_0^2 + (3p_i - \rho^2)}{\rho^2}K(k_i) \\ -\frac{3(r_0 - \rho)r_0^2}{(r_0 + \rho)\rho^2}\Pi(n, k_i) \end{bmatrix}$$
$$\text{for } \rho \neq r_0 \text{ and } \rho \neq 0 \tag{72d}$$

in which $K(k)$ and $E(k)$ are the complete elliptic integrals of the first and second kinds with modulus k, and $\Pi(n, k)$ is the complete elliptic integral of the third kind with modulus k and parameter n, and (Khraishi et al., 2000)

$$\begin{aligned} &R_i = \sqrt{p_i - q\cos\varphi},\ \ r_{\mathrm{pn}} = \sqrt{s - q\cos\varphi}, \\ &n = 2q/(s + q),\ \ k_i = \sqrt{2q/(p_i + q)}, \\ &p_i = s + x_3^2/\gamma_i^2,\ \ q = 2\rho r_0,\ \ s = \rho^2 + r_0^2, \\ &\rho = \sqrt{x_1^2 + x_2^2},\ \ \theta = \arctan(x_2/x_1). \end{aligned} \tag{73}$$

During the derivation of Eq. (69a), use has been made of the following relation

$$\rho^2\frac{\partial I_{2i}}{\partial\rho} = \frac{\partial(\rho^2 I_{3i})}{\partial\rho} \tag{74}$$

which can be proved by direct substitution.

We remark that Eqs. (71a)–(72d) are also applicable to the trivial case of $\rho = r_0$, provided that all the terms involving $\Pi(n, k_i)$

vanish. For the trivial case of $\rho = 0$, the integrals in Eqs. (71a)–(72d) can be integrated directly and the results are omitted here due to its simplicity. Furthermore, when $\rho = 0$, Eqs. (68a)–(69c) are valid, provided that all the terms involving I_{3i}/ρ and J_{4i}/ρ vanish, which can be verified by utilizing the L'Hopital's rule when $\rho \to 0$. We finally remark that our new solutions given in Eqs. (68a)–(69c) are mathematically identical to those derived by Ohr (1972, 1973); however, our solutions are more explicit, and are applicable to arbitrary field points.

8. Numerical examples and discussions

In this section, our explicit solutions are applied to a couple of dislocation cases to verify their accuracy while illustrating certain interesting features we pointed out in previous sections.

Example 1: The quasi solid angle Ω_3 of a planar triangle *ABC*.

In this example, the quasi solid angle Ω_3 is investigated by virtue of Eq. (66). In Cartesian coordinates (x_1, x_2, x_3), Fig. 4 shows the variation of Ω_3 with x_3 for a generally oriented planar triangle *ABC*, with its three vertices being at dimensionless locations *A*(3,0,0), *B*(0,2,1) and *C*(0,0,3). Fig. 5 shows the variation of Ω_3 with x_1 for a planar triangle *ABC*, with its positive normal in the x_1-direction and its vertices at dimensionless locations *A*(0,0,0), *B*(0,2,1), and *C*(0,0,3). As verification, the traditional solid angle Ω of a planar triangle *ABC* is also calculated by simply setting $\gamma_3 = 1$ in Eq. (66), and the numerical results are compared with those by Oosterom and Strackee (1983). It is clear from Figs. 4 and 5 that Eq. (66) is accurate. Moreover, the discontinuities in these two figures are clearly illustrated by our expression (66): The discontinuities at $x_3 = 1$ in Fig. 4 are totally due to the function Φ, while those at $x_1 = 0$ in Fig. 5 are due to the remaining part on the right-hand side of Eq. (66). The effect of γ_3 on Ω_3 is also observed from these figures.

Example 2: A glide circular dislocation loop parallel to the plane of isotropy.

For this problem, on the one hand, the analytical solution in terms of complete elliptic integrals is available, as given in Section 7 of this paper and in Ohr (1973). On the other hand, a circular loop can be approximated with arbitrary accuracy by a series of end-to-end connected straight dislocation segments. Therefore, this will help verify our solutions for both circular dislocation loops and straight dislocation segments.

Shown in Figs. 6 and 7 are, respectively, the displacement component u_1 and the stress component σ_{13} produced by a glide circular dislocation loop of radius r_0 (=50*b*) with its centre being

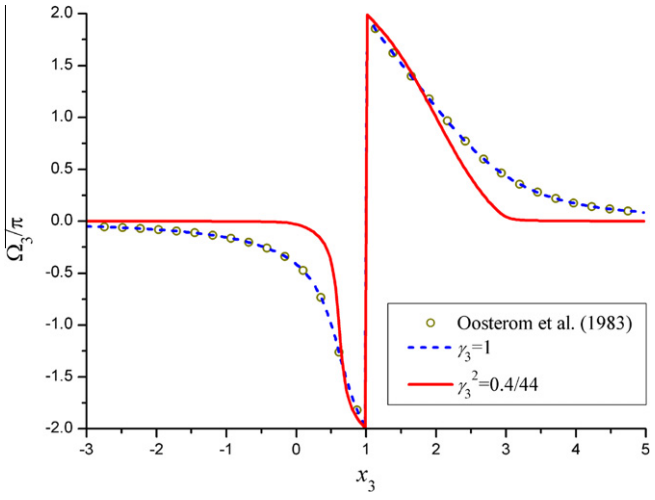

Fig. 4. Variation of Ω_3 of a generally oriented triangle *ABC* with x_3 ($x_1 = 1$, $x_2 = 1$).

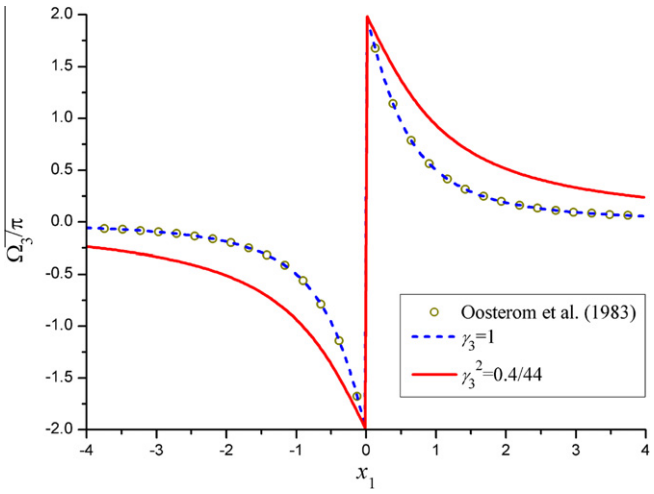

Fig. 5. Variation of Ω_3 of a specially oriented triangle *ABC* with x_1 ($x_2 = 1$, $x_3 = 1$).

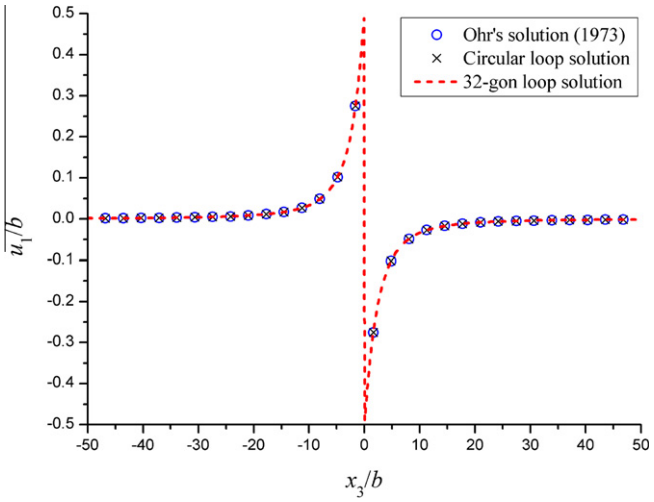

Fig. 6. Comparison of the displacement component u_1 among our circular loop solution, our 32-gon loop solution, and Ohr's solution (with fixed $x_1/b = 25$, $x_2/b = 0$).

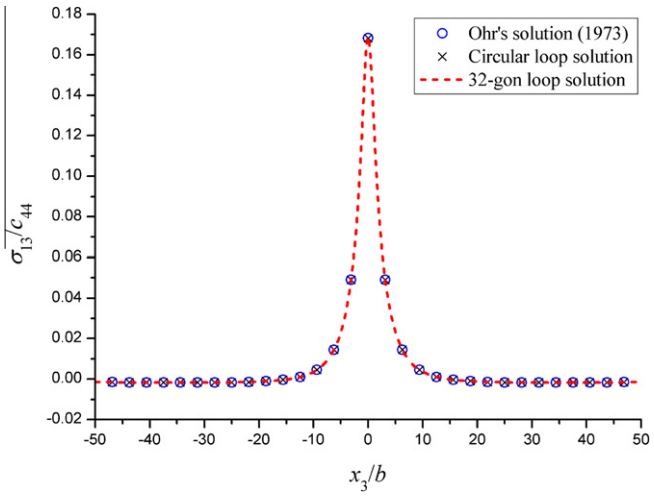

Fig. 7. Comparison of the stress component σ_{13} among our circular loop solution, our 32-gon loop solution, and Ohr's solution (with fixed $x_1/b = 25$, $x_2/b = 0$).

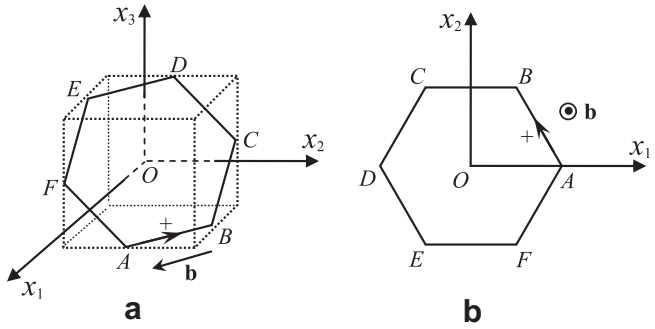

Fig. 8. (a) An inclined, planar hexagonal dislocation loop. (b) A planar prismatic hexagonal dislocation loop parallel to the plane of isotropy.

at (0,0,0), subjected to a constant Burgers vector (b,0,0) on its face. When applying the straight segment solution, an inscribed regular 32-side polygon is used to approximate such a circle. It is observed from Figs. 6 and 7 that, the numerical results of our polygonal loop solution in terms of the straight segment solutions, i.e., (35a)–(36c) plus (39) and (40), are in good agreement with those of our circular loop solution (68a)–(69c) and those of Ohr's solution. For other displacement and stress components, the numerical results via these three different approaches also agree well with each other. The elastic stiffness constants of transverse isotropy used here, as well as in the subsequent Examples 3 and 4, are those of graphite (Ohr, 1973), namely, $c_{11} = 106$, $c_{33} = 3.65$, $c_{44} = 0.4$, $c_{13} = 1.5$, $c_{66} = 44$ (10^{11} dyn/cm^2). The corresponding isotropic Lamé constants used in Example 3 below are $\lambda = 14.00$, $\mu = 21.94$ (10^{11} dyn/cm^2), which are determined by the Voigt average for graphite (Hirth and Lothe, 1982). We also remark that all the results presented in Example 2, 3 and 4 are dimensionless.

Example 3: An inclined, planar hexagonal dislocation loop.

In this Example 3, we consider an inclined, planar hexagonal dislocation loop *ABCDEF* subjected to a constant Burgers vector $(b/\sqrt{2}, -b/\sqrt{2}, 0)$ on its face, with the six vertices being at $A(a, 0, -a)$, $B(0, a, -a)$, $C(-a, a, 0)$, $D(-a, 0, a)$, $E(0, -a, a)$, $F(a, -a, 0)$ where $a = 50b$, as shown in Fig. 8a. Fig. 8b is needed in the next example.

The induced displacement and stress components are evaluated based on our exact closed-form solutions (28a)–(29c) plus (39) and (40) for a single straight line segment, along with the method of superposition. The results are shown in Figs. 9 and 10 in local Cartesian coordinates (x_1', x_2', x_3'), with the local unit basis vectors being

$$\mathbf{i}' = (1, -1, 0)/\sqrt{2}, \quad \mathbf{j}' = (1, 1, -2)/\sqrt{6}, \quad \mathbf{k}' = (1, 1, 1)/\sqrt{3} \tag{75}$$

Only the non-zero components of displacements and stresses are depicted here. It is observed from Figs. 9 and 10 that, while the dislocation-induced displacements are very close to each other

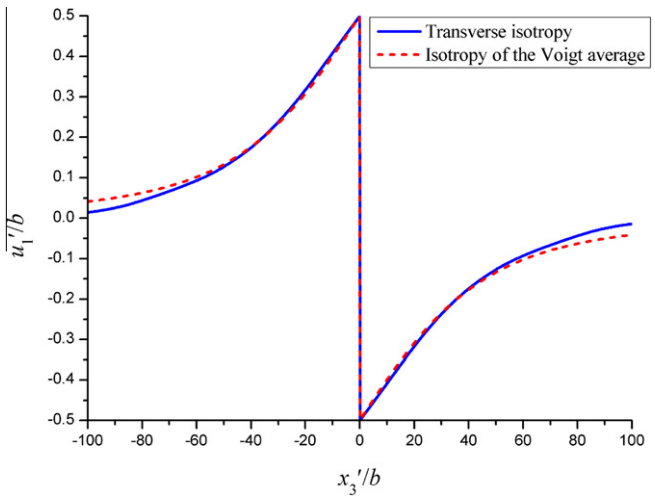

Fig. 9. The non-zero displacements in local coordinates due to an inclined, planar hexagonal dislocation loop *ABCDEF* (with fixed $x_1'/b = 0$, $x_2'/b = 0$).

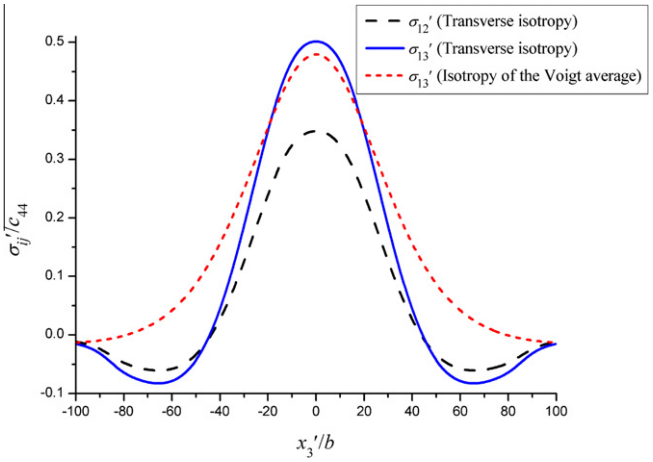

Fig. 10. The non-zero stresses in local coordinates due to an inclined, planar hexagonal dislocation loop *ABCDEF* (with fixed $x_1'/b = 0$, $x_2'/b = 0$).

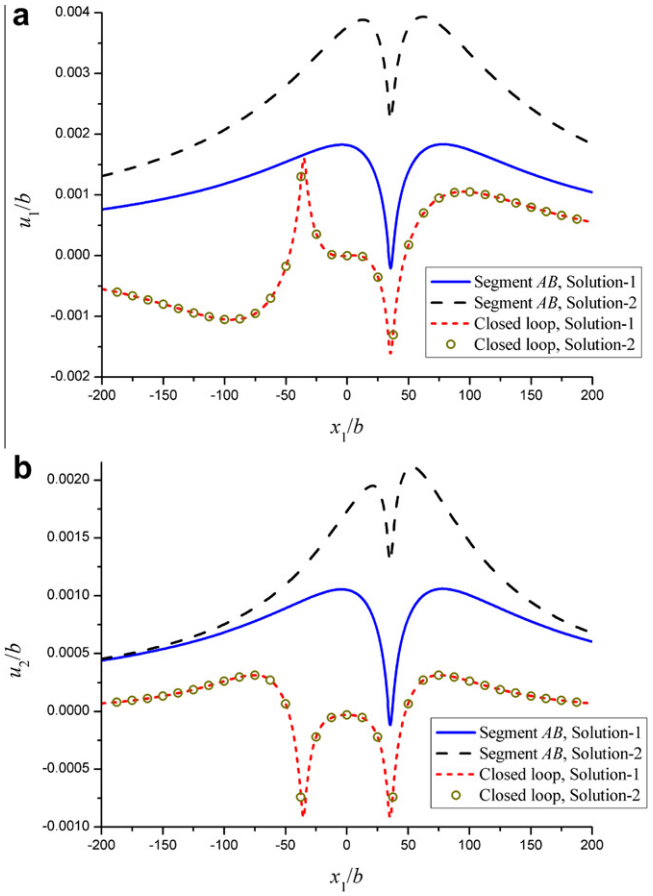

Fig. 11. The displacements (u_1 in (a) and u_2 in (b)) due to one side *AB* of a prismatic hexagonal loop parallel to the plane of isotropy and due to the closed loop (with fixed $x_2/b = 25$, $x_3/b = 5$).

in the transversely isotropic and isotropic full spaces, the induced stresses in these two full spaces are very different. Furthermore, due to the material anisotropy, an extra shear stress component σ_{12} is introduced, apart from the stress component σ_{13} which is also observed in the isotropic full space.

Example 4: Non-uniqueness of the elastic field of a straight dislocation segment.

To illustrate the non-uniqueness of the displacement and stress fields due to a straight dislocation segment, we consider a planar hexagonal dislocation loop of side-length a parallel to the plane of isotropy, with its six vertices being at $A(a,0,0)$, $B(a/2,\sqrt{3}a/2,0)$, $C(-a/2,\sqrt{3}a/2,0)$, $D(-a,0,0)$, $E(-a/2,-\sqrt{3}a/2,0)$ and $F(a/2,-\sqrt{3}a/2,0)$, as shown in Fig. 8b. Since the introduction of the three integral identities (27a–c) only changes the form of the elastic field solution related to the third component of **b**, a prismatic loop with Burgers vector (0,0,b) is studied here ($a = 50b$), and we focus only on the representative segment AB of this loop in our discussion.

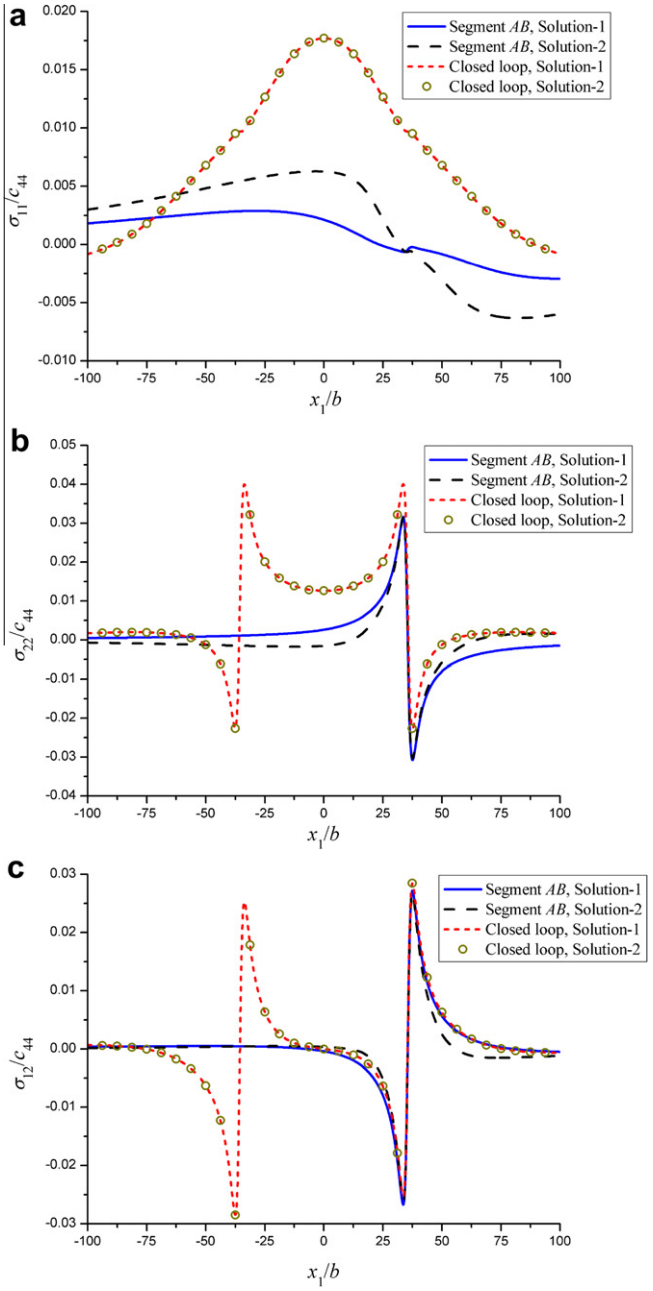

Fig. 12. The stresses (σ_{11} in (a), σ_{22} in (b), and σ_{12} in (c)) due to one side AB of a prismatic hexagonal loop parallel to the plane of isotropy and due to the closed loop (with fixed $x_2/b = 25$, $x_3/b = 5$).

Two types of infinitesimal dislocation line element, corresponding to two different line-integral representations of the elastic field due to an arbitrary dislocation loop, are adopted to develop the straight dislocation segment solutions, i.e.,

Solution-1: the one corresponding to Eqs. (28a)–(29c), and

Solution-2: the one constructed by re-substituting Eq. (27c) into Eq. (28a), Eq. (27a) into Eq. (29a), and Eq. (27b) into Eq. (29b). Note that u_3 and σ_{33} are not affected by this procedure, thus will not be discussed below.

The numerical results for the displacement and stress fields based on these two different solutions are shown in Figs. 11 and 12. It is observed that, the displacements and stresses due to the single segment AB based on Solution-1 are obviously different from those based on Solution-2; however, for the closed planar hexagonal loop, both solutions predict the same unique elastic field, no matter which kind of dislocation line element is utilized to construct this closed loop. We also point out that, since the stresses $\sigma_{\alpha 3}$ due to segment AB based on these two solutions differ from each other only slightly, the corresponding curves are omitted.

9. Conclusions

In this paper, we have derived a simple line-integral representation of the displacement and stress fields due to an arbitrary dislocation loop in a transversely isotropic elastic full space. In the case of transverse isotropy, our displacement formulae are simpler and more explicit than Indenbom and Orlov's formula (Hirth and Lothe, 1982), and our stress formulae are simpler and more efficient than Mura's formula (Hirth and Lothe, 1982). Particularly, we apply our line-integral solution for dislocation loops to a straight dislocation segment of arbitrary orientation, and for the first time we express both the induced displacements and stresses uniformly in terms of elementary functions. Meanwhile, we rigorously demonstrate the non-uniqueness of the elastic field due to an open dislocation segment. We further give a new explicit formula for calculating accurately and efficiently the traditional solid angle of an arbitrary polygonal dislocation loop. For a circular dislocation loop parallel to the plane of isotropy, a new explicit expression of the induced elastic field is also presented in terms of complete elliptic integrals, which is valid for arbitrary field points.

Unlike the previous treatment of the corresponding isotropic case in the literature, we have introduced three quasi solid angles to describe the displacement discontinuities over the dislocation surface in a transversely isotropic full space. Based on a convenient line integral representation of the quasi solid angle, we are able to extract a simple and intuitive step function to characterize the dependence of the displacements on the configuration of the dislocation surface. Further, we conclude that, for any complex assembly of dislocation loops which is entirely located within a finite cylinder normal to the plane of isotropy, the induced displacement field outside the cylinder can be totally determined by the integration over the closed dislocation lines, independent of the dislocation surface configurations inside.

We finally point out that, from the present line-integral representation for a finite dislocation loop, a closed-form solution for an infinitesimal dislocation loop can also be achieved by the limiting process, which is useful in developing numerical solutions of 3D crack problems via the distributed dislocation technique (Hills et al., 1996). The present approach is also applicable to infinite straight dislocations of arbitrary orientation, provided that one calculates the involved divergent integrals properly in the finite-part sense.

Acknowledgments

Professor Y.H. Pao from College of Civil Engineering and Architecture at Zhejiang University is greatly acknowledged. This work is supported by the National Project of Scientific and Technical Supporting Programs Funded by Ministry of Science & Technology of China (No. 2009BAG12A01-A03-2) and the National Basic Research Program of China (No. 2009CB623204). It is also partly supported by the National Natural Science Foundation of China (Nos. 10972196, 11090333, 11172273).

Appendix A. A straight dislocation segment normal to the plane of isotropy

Corresponding to Case 1 in Section 6, the line integrals required in Eqs. (43a)–(44c) are listed as follows

$$\vec{I}^{\sim}_{N;m3}=\frac{(x_{3B}-x_{3A})}{d^N_{\rm pn}}\int_0^1\frac{{\rm d}t}{R_m}\quad(N=0,2,4)$$

$$\vec{I}^{3}_{N;m3}=\frac{(x_{3B}-x_{3A})^2}{d^N_{\rm pn}}\left[\frac{1}{l_m^2}R_m|_0^1+\left(T_m-\frac{x_3-x_{3A}}{x_{3B}-x_{3A}}\right)\int_0^1\frac{{\rm d}t}{R_m}\right]\quad(N=2,4)$$

$$\vec{I}^{33}_{N;m3}=\frac{(x_{3B}-x_{3A})^3}{d^N_{\rm pn}}\left\{\begin{array}{l}\frac{2}{l_m^2}\left(T_m-\frac{x_3-x_{3A}}{x_{3B}-x_{3A}}\right)R_m|_0^1+\frac{1}{2l_m^2}[(t-T_m)R_m]|_0^1\\+\left[(T_m-\frac{x_3-x_{3A}}{x_{3B}-x_{3A}})^2-\frac{1}{2}(D_m^2-T_m^2)\right]\int_0^1\frac{{\rm d}t}{R_m}\end{array}\right\}$$
$$(N=2,4,6)\qquad\text{(A1)}$$

and

$$\vec{J}^{\sim}_{N;m3}=\frac{(x_{3B}-x_{3A})}{d^N_{\rm pn}}\int_0^1\frac{{\rm d}t}{R_m^3}\quad(N=0,2)$$

$$\vec{J}^{3}_{N;m3}=\frac{(x_{3B}-x_{3A})^2}{d^N_{\rm pn}}\left[-\frac{1}{l_m^2}(1/R_m)|_0^1+\left(T_m-\frac{x_3-x_{3A}}{x_{3B}-x_{3A}}\right)\int_0^1\frac{{\rm d}t}{R_m^3}\right]\quad(N=0,2)\qquad\text{(A2)}$$

The integrals in Eq. (46) are also needed here.

Appendix B. A straight dislocation segment parallel to the plane of isotropy

Corresponding to Case 2 in Section 6, the line integrals required in Eqs. (35a)–(36c) are listed as follows

$$\vec{I}^{\sim}_{0;m\kappa}=(x_{\kappa B}-x_{\kappa A})\int_0^1\frac{{\rm d}t}{R_m};\quad\vec{I}^{\sim}_{2;m\kappa}=\frac{(x_{\kappa B}-x_{\kappa A})}{l^2_{\rm pn}}\int_0^1\frac{{\rm d}t}{\Upsilon^2_{\rm pn}R_m}$$

$$\vec{I}^{\alpha}_{2;m\kappa}=\frac{(x_{\kappa B}-x_{\kappa A})}{l^2_{\rm pn}}\int_0^1\frac{(x_{\alpha B}-x_{\alpha A})t-(x_\alpha-x_{\alpha A})}{\Upsilon^2_{\rm pn}R_m}{\rm d}t$$

$$\vec{I}^{\xi\eta}_{4;m\kappa}=\frac{(x_{\kappa B}-x_{\kappa A})}{l^4_{\rm pn}}\left[(x_{\xi B}-x_{\xi A})(x_{\eta B}-x_{\eta A})\int_0^1\frac{1}{\Upsilon^2_{\rm pn}R_m}{\rm d}t+\int_0^1\frac{\Gamma_1 t+\Gamma_0}{\Upsilon^4_{\rm pn}R_m}{\rm d}t\right]\qquad\text{(B1)}$$

and

$$\vec{J}^{\sim}_{0;m\kappa}=(x_{\kappa B}-x_{\kappa A})\int_0^1\frac{{\rm d}t}{R_m^3}$$

$$\vec{J}^{\alpha}_{0;m\kappa}=(x_{\kappa B}-x_{\kappa A})\left\{-\frac{(x_{\alpha B}-x_{\alpha A})}{l_m^2}(1/R_m)|_0^1+[(x_{\alpha B}-x_{\alpha A})T_m-(x_\alpha-x_{\alpha A})]\int_0^1\frac{{\rm d}t}{R_m^3}\right\}$$

$$\vec{J}^{\xi\eta}_{2;m\kappa}=\frac{(x_{\kappa B}-x_{\kappa A})}{l^2_{\rm pn}}\left[(x_{\xi B}-x_{\xi A})(x_{\eta B}-x_{\eta A})\int_0^1\frac{{\rm d}t}{R_m^3}+\int_0^1\frac{\Gamma_1 t+\Gamma_0}{\Upsilon^2_{\rm pn}R_m^3}{\rm d}t\right]\qquad\text{(B2)}$$

where

$$\begin{aligned}\Gamma_1&=2(x_{\xi B}-x_{\xi A})(x_{\eta B}-x_{\eta A})T_{\rm pn}-(x_\xi-x_{\xi A})(x_{\eta B}-x_{\eta A})\\&\quad-(x_{\xi B}-x_{\xi A})(x_\eta-x_{\eta A})\\\Gamma_0&=(x_\xi-x_{\xi A})(x_\eta-x_{\eta A})-(x_{\xi B}-x_{\xi A})(x_{\eta B}-x_{\eta A})D^2_{\rm pn}\end{aligned}\qquad\text{(B3)}$$

Again, the integrals in Eq. (46) are needed in Eqs. (B1) and (B2). Meanwhile, we also need to evaluate the integrals of the form

$$\begin{aligned}\int_0^1\frac{\hat\Gamma_1 t+\hat\Gamma_0}{\Upsilon^N_{\rm pn}R^Z_m}{\rm d}t&=\int_{\tau_0}^{\tau_1}\frac{(\hat\Gamma_1)\tau{\rm d}\tau}{(\lambda_{\rm pn}+\tau^2)^{N/2}[l_m^2(\lambda_m+\tau^2)]^{Z/2}}\\&\quad+\int_{\tau_0}^{\tau_1}\frac{(T_{\rm pn}\hat\Gamma_1+\hat\Gamma_0){\rm d}\tau}{(\lambda_{\rm pn}+\tau^2)^{N/2}[l_m^2(\lambda_m+\tau^2)]^{Z/2}}\end{aligned}\qquad\text{(B4)}$$

where τ_0, τ_1, $\lambda_{\rm pn}$, λ_m are defined in Eq. (51), and the following integrals are involved

$$\int\frac{\tau{\rm d}\tau}{(\lambda_{\rm pn}+\tau^2)[l_m^2(\lambda_m+\tau^2)]^{1/2}}=\frac{\sqrt{l_m^2(\lambda_m-\lambda_{\rm pn})}}{2l_m^2(\lambda_m-\lambda_{\rm pn})}\ln\frac{\xi-1}{\xi+1}\quad\text{for }\lambda_m\neq\lambda_{\rm pn}$$

$$\int\frac{\tau{\rm d}\tau}{(\lambda_{\rm pn}+\tau^2)^2[l_m^2(\lambda_m+\tau^2)]^{1/2}}=-\frac{\sqrt{l_m^2(\lambda_m-\lambda_{\rm pn})}}{2l_m^2(\lambda_m-\lambda_{\rm pn})^2}\left(\frac{1}{2}\ln\frac{\xi-1}{\xi+1}+\frac{\xi}{\xi^2-1}\right)\quad\text{for }\lambda_m\neq\lambda_{\rm pn}$$

$$\int\frac{\tau{\rm d}\tau}{(\lambda_{\rm pn}+\tau^2)[l_m^2(\lambda_m+\tau^2)]^{3/2}}=\frac{\sqrt{l_m^2(\lambda_m-\lambda_{\rm pn})}}{l_m^4(\lambda_m-\lambda_{\rm pn})^2}\left(\frac{1}{2}\ln\frac{\xi-1}{\xi+1}+\frac{1}{\xi}\right)\quad\text{for }\lambda_m\neq\lambda_{\rm pn}\qquad\text{(B5)}$$

and

$$\int\frac{{\rm d}\tau}{(\lambda_{\rm pn}+\tau^2)[l_m^2(\lambda_m+\tau^2)]^{1/2}}=\frac{1}{\lambda_{\rm pn}^{1/2}\sqrt{l_m^2(\lambda_m-\lambda_{\rm pn})}}\arctan\zeta\quad\text{for }\lambda_m\neq\lambda_{\rm pn},\ \lambda_{\rm pn}\neq0$$

$$\int\frac{{\rm d}\tau}{(\lambda_{\rm pn}+\tau^2)^2[l_m^2(\lambda_m+\tau^2)]^{1/2}}=\frac{l_m^2}{2\lambda_{\rm pn}^{3/2}[l_m^2(\lambda_m-\lambda_{\rm pn})]^{3/2}}\left[(\lambda_m-2\lambda_{\rm pn})\arctan\zeta+\lambda_m\frac{\zeta}{\zeta^2+1}\right]\quad\text{for }\lambda_m\neq\lambda_{\rm pn},\ \lambda_{\rm pn}\neq0$$

$$\int\frac{{\rm d}\tau}{(\lambda_{\rm pn}+\tau^2)[l_m^2(\lambda_m+\tau^2)]^{3/2}}=\frac{\lambda_m\arctan\zeta-\lambda_{\rm pn}\zeta}{\lambda_m\lambda_{\rm pn}^{1/2}[l_m^2(\lambda_m-\lambda_{\rm pn})]^{3/2}}\quad\text{for }\lambda_m\neq\lambda_{\rm pn},\ \lambda_{\rm pn}\neq0\qquad\text{(B6)}$$

with ξ and ζ defined in Eq. (53). The trivial case of $\lambda_m=\lambda_{\rm pn}$ or $\lambda_{\rm pn}=0$ is omitted here.

Appendix C. A straight dislocation segment neither normal nor parallel to the plane of isotropy

The line integrals required in Eqs. (28a)–(29c) for Case 3 are listed as follows

$$\vec{\tilde{\mathrm{I}}}_{0;mk}=(x_{kB}-x_{kA})\int_0^1\frac{\mathrm{d}t}{R_m};$$

$$\vec{\mathrm{I}}^{i}_{2;mk}=\frac{(x_{kB}-x_{kA})}{l_{\mathrm{pn}}^2}\int_0^1\frac{(x_{iB}-x_{iA})t-(x_i-x_{iA})}{\Upsilon_{\mathrm{pn}}^2R_m}\mathrm{d}t$$

$$\vec{\mathrm{I}}^{ij}_{2;mk}=\frac{(x_{kB}-x_{kA})}{l_{\mathrm{pn}}^2}\left(\Gamma_{00}\int_0^1\frac{\mathrm{d}t}{R_m}+\int_0^1\frac{\Gamma_{11}t+\Gamma_{10}}{\Upsilon_{\mathrm{pn}}^2R_m}\mathrm{d}t\right)$$

$$\vec{\mathrm{I}}^{ijl}_{4;mk}=\frac{(x_{kB}-x_{kA})}{l_{\mathrm{pn}}^4}\left(\int_0^1\frac{\Gamma_{21}t+\Gamma_{20}}{\Upsilon_{\mathrm{pn}}^2R_m}\mathrm{d}t+\int_0^1\frac{\Gamma_{31}t+\Gamma_{30}}{\Upsilon_{\mathrm{pn}}^4R_m}\mathrm{d}t\right)$$

$$\vec{\mathrm{I}}^{ij33}_{4;mk}=\frac{(x_{kB}-x_{kA})}{l_{\mathrm{pn}}^4}\left(\Lambda_{00}\Gamma_{00}\int_0^1\frac{\mathrm{d}t}{R_m}+\int_0^1\frac{\Gamma_{41}t+\Gamma_{40}}{\Upsilon_{\mathrm{pn}}^2R_m}\mathrm{d}t+\int_0^1\frac{\Gamma_{51}t+\Gamma_{50}}{\Upsilon_{\mathrm{pn}}^4R_m}\mathrm{d}t\right)$$

$$\vec{\mathrm{I}}^{ijl33}_{6;mk}=\frac{(x_{kB}-x_{kA})}{l_{\mathrm{pn}}^6}\left(\int_0^1\frac{\Gamma_{61}t+\Gamma_{60}}{\Upsilon_{\mathrm{pn}}^2R_m}\mathrm{d}t+\int_0^1\frac{\Gamma_{71}t+\Gamma_{70}}{\Upsilon_{\mathrm{pn}}^4R_m}\mathrm{d}t+\int_0^1\frac{\Gamma_{81}t+\Gamma_{80}}{\Upsilon_{\mathrm{pn}}^6R_m}\mathrm{d}t\right)\tag{C1}$$

and

$$\vec{\mathrm{J}}^{i}_{0;mk}=(x_{kB}-x_{kA})\left\{-\frac{(x_{iB}-x_{iA})}{l_m^2}(1/R_m)\big|_0^1+[T_m(x_{iB}-x_{iA})-(x_i-x_{iA})]\int_0^1\frac{\mathrm{d}t}{R_m^3}\right\}$$

$$\vec{\mathrm{J}}^{ijl}_{2;mk}=\frac{(x_{kB}-x_{kA})}{l_{\mathrm{pn}}^2}\left[\int_0^1\frac{\Gamma_{31}t+\Gamma_{30}}{\Upsilon_{\mathrm{pn}}^2R_m^3}\mathrm{d}t-\frac{\Gamma_{21}}{l_m^2}(1/R_m)\big|_0^1+(T_m\Gamma_{21}+\Gamma_{20})\int_0^1\frac{\mathrm{d}t}{R_m^3}\right]\tag{C2}$$

where

$$\Gamma_{00}=(x_{iB}-x_{iA})(x_{jB}-x_{jA})$$

$$\Gamma_{10}=-D_{\mathrm{pn}}^2\Gamma_{00}+(x_i-x_{iA})(x_j-x_{jA})$$

$$\Gamma_{11}=2T_{\mathrm{pn}}\Gamma_{00}-[(x_i-x_{iA})(x_{jB}-x_{jA})+(x_{iB}-x_{iA})(x_j-x_{jA})]$$

$$\Lambda_{00}=(x_{3B}-x_{3A})^2$$

$$\Lambda_{10}=-D_{\mathrm{pn}}^2\Lambda_{00}+(x_3-x_{3A})^2$$

$$\Lambda_{11}=2T_{\mathrm{pn}}\Lambda_{00}-2(x_{3B}-x_{3A})(x_3-x_{3A})$$

$$\Gamma_{21}=(x_{iB}-x_{iA})(x_{jB}-x_{jA})(x_{lB}-x_{lA})$$

$$\Gamma_{20}=2T_{\mathrm{pn}}\Gamma_{21}-\begin{bmatrix}+(x_i-x_{iA})(x_{jB}-x_{jA})(x_{lB}-x_{lA})\\+(x_{iB}-x_{iA})(x_j-x_{jA})(x_{lB}-x_{lA})\\+(x_{iB}-x_{iA})(x_{jB}-x_{jA})(x_l-x_{lA})\end{bmatrix}$$

$$\Gamma_{31}=2T_{\mathrm{pn}}\Gamma_{20}-D_{\mathrm{pn}}^2\Gamma_{21}+\begin{bmatrix}+(x_{iB}-x_{iA})(x_j-x_{jA})(x_l-x_{lA})\\+(x_i-x_{iA})(x_{jB}-x_{jA})(x_l-x_{lA})\\+(x_i-x_{iA})(x_j-x_{jA})(x_{lB}-x_{lA})\end{bmatrix}$$

$$\Gamma_{30}=-D_{\mathrm{pn}}^2\Gamma_{20}-(x_i-x_{iA})(x_j-x_{jA})(x_l-x_{lA})$$

$$\Gamma_{41}=\Gamma_{11}\Lambda_{00}+\Gamma_{00}\Lambda_{11};\quad \Gamma_{40}=\Gamma_{11}\Lambda_{11}+\Gamma_{10}\Lambda_{00}+\Gamma_{00}\Lambda_{10}$$

$$\Gamma_{51}=2T_{\mathrm{pn}}\Gamma_{11}\Lambda_{11}+\Gamma_{11}\Lambda_{10}+\Gamma_{10}\Lambda_{11};$$

$$\Gamma_{50}=-D_{\mathrm{pn}}^2\Gamma_{11}\Lambda_{11}+\Gamma_{10}\Lambda_{10}$$

$$\Gamma_{61}=\Gamma_{21}\Lambda_{00};\quad \Gamma_{60}=\Gamma_{21}\Lambda_{11}+\Gamma_{20}\Lambda_{00}$$

$$\Gamma_{71}=\Gamma_{31}\Lambda_{00}+\Gamma_{21}\Lambda_{10}+(2T_{\mathrm{pn}}\Gamma_{21}+\Gamma_{20})\Lambda_{11}$$

$$\Gamma_{70}=(\Gamma_{31}-D_{\mathrm{pn}}^2\Gamma_{21})\Lambda_{11}+\Gamma_{30}\Lambda_{00}+\Gamma_{20}\Lambda_{10}$$

$$\Gamma_{81}=\Gamma_{31}(2T_{\mathrm{pn}}\Lambda_{11}+\Lambda_{10})+\Gamma_{30}\Lambda_{11};$$

$$\Gamma_{80}=-D_{\mathrm{pn}}^2\Gamma_{31}\Lambda_{11}+\Gamma_{30}\Lambda_{10}\tag{C3}$$

When $[\mathbf{l}_m\times(\mathbf{d}_m\times\mathbf{l}_m)]\cdot\mathbf{k}=0$, i.e., $T_m=T_{\mathrm{pn}}$, we need Eq. (46), Eqs. (B4)–(B6) and the following integrals

$$\int\frac{\tau\mathrm{d}\tau}{(\lambda_{\mathrm{pn}}+\tau^2)^3[l_m^2(\lambda_m+\tau^2)]^{1/2}}=\frac{l_m^4}{[l_m^2(\lambda_m-\lambda_{\mathrm{pn}})]^{5/2}}\times\left[\frac{3}{16}\ln\frac{\xi-1}{\xi+1}+\frac{3}{8}\frac{\xi}{\xi^2-1}-\frac{1}{4}\frac{\xi}{(\xi^2-1)^2}\right]\ \text{for}\ \lambda_m\neq\lambda_{\mathrm{pn}}$$

$$\int\frac{\tau\mathrm{d}\tau}{[l_m^2(\lambda_m+\tau^2)]^{3/2}}=-\frac{1}{l_m^2}\frac{1}{[l_m^2(\lambda_m+\tau^2)]^{1/2}}\tag{C4}$$

and

$$\int\frac{\mathrm{d}\tau}{(\lambda_{\mathrm{pn}}+\tau^2)^3[l_m^2(\lambda_m+\tau^2)]^{1/2}}=\frac{l_m^4}{\lambda_{\mathrm{pn}}^{5/2}[l_m^2(\lambda_m-\lambda_{\mathrm{pn}})]^{5/2}}\times\begin{bmatrix}(\frac{3}{8}\lambda_m^2-\lambda_{\mathrm{pn}}\lambda_m)\frac{\zeta}{\zeta^2+1}+\frac{1}{4}\lambda_m^2\frac{\zeta}{(\zeta^2+1)^2}\\+(\frac{3}{8}\lambda_m^2-\lambda_{\mathrm{pn}}\lambda_m+\lambda_{\mathrm{pn}}^2)\arctan\zeta\end{bmatrix}\ \text{for}\ \lambda_m\neq\lambda_{\mathrm{pn}},\ \lambda_{\mathrm{pn}}\neq0$$

$$\int\frac{\mathrm{d}\tau}{[l_m^2(\lambda_m+\tau^2)]^{3/2}}=\frac{1}{l_m^2\lambda_m}\frac{\tau}{\sqrt{l_m^2(\lambda_m+\tau^2)}}\ \text{for}\ \lambda_m\neq0\tag{C5}$$

with ξ and ζ being defined in Eq. (53). Again, the trivial case of $\lambda_m=\lambda_{\mathrm{pn}}$ or $\lambda_{\mathrm{pn}}=0$ is omitted here.

When $[\mathbf{l}_m\times(\mathbf{d}_m\times\mathbf{l}_m)]\cdot\mathbf{k}\neq0$, i.e., $T_m\neq T_{\mathrm{pn}}$, we need the following integrals

$$\int_0^1\frac{\hat{\Gamma}_1t+\hat{\Gamma}_0}{\Upsilon_{\mathrm{pn}}^2R_m}\mathrm{d}t=\frac{2\varpi_2}{\lambda_{\mathrm{pn}}^+}\int_{\tau_0}^{\tau_1}\frac{(\Theta_{11}\tau+\Theta_{10})\mathrm{sgn}\langle\tau+1\rangle}{(\lambda_{\mathrm{pn}}+\tau^2)[(l_m^2\lambda_m^+)(\lambda_m+\tau^2)]^{1/2}}\mathrm{d}\tau$$

$$\int_0^1\frac{\hat{\Gamma}_1t+\hat{\Gamma}_0}{\Upsilon_{\mathrm{pn}}^4R_m}\mathrm{d}t=\frac{2\varpi_2}{(\lambda_{\mathrm{pn}}^+)^2}\begin{bmatrix}+\int_{\tau_0}^{\tau_1}\frac{(\Theta_{21}\tau+\Theta_{20})\mathrm{sgn}\langle\tau+1\rangle}{(\lambda_{\mathrm{pn}}+\tau^2)[(l_m^2\lambda_m^+)(\lambda_m+\tau^2)]^{1/2}}\mathrm{d}\tau\\+\int_{\tau_0}^{\tau_1}\frac{(\Theta_{31}\tau+\Theta_{30})\mathrm{sgn}\langle\tau+1\rangle}{(\lambda_{\mathrm{pn}}+\tau^2)^2[(l_m^2\lambda_m^+)(\lambda_m+\tau^2)]^{1/2}}\mathrm{d}\tau\end{bmatrix}$$

$$\int_0^1\frac{\hat{\Gamma}_1t+\hat{\Gamma}_0}{\Upsilon_{\mathrm{pn}}^6R_m}\mathrm{d}t=\frac{2\varpi_2}{(\lambda_{\mathrm{pn}}^+)^3}\begin{bmatrix}+\int_{\tau_0}^{\tau_1}\frac{(\Theta_{41}\tau+\Theta_{40})\mathrm{sgn}\langle\tau+1\rangle}{(\lambda_{\mathrm{pn}}+\tau^2)[(l_m^2\lambda_m^+)(\lambda_m+\tau^2)]^{1/2}}\mathrm{d}\tau\\+\int_{\tau_0}^{\tau_1}\frac{(\Theta_{51}\tau+\Theta_{50})\mathrm{sgn}\langle\tau+1\rangle}{(\lambda_{\mathrm{pn}}+\tau^2)^2[(l_m^2\lambda_m^+)(\lambda_m+\tau^2)]^{1/2}}\mathrm{d}\tau\\+\int_{\tau_0}^{\tau_1}\frac{(\Theta_{61}\tau+\Theta_{60})\mathrm{sgn}\langle\tau+1\rangle}{(\lambda_{\mathrm{pn}}+\tau^2)^3[(l_m^2\lambda_m^+)(\lambda_m+\tau^2)]^{1/2}}\mathrm{d}\tau\end{bmatrix}$$

$$\int_0^1\frac{\hat{\Gamma}_1t+\hat{\Gamma}_0}{\Upsilon_{\mathrm{pn}}^2R_m^3}\mathrm{d}t=\frac{2\varpi_2}{\lambda_{\mathrm{pn}}^+}\begin{bmatrix}+\int_{\tau_0}^{\tau_1}\frac{(\Theta_{21}\tau+\Theta_{20})\mathrm{sgn}\langle\tau+1\rangle}{[(l_m^2\lambda_m^+)(\lambda_m+\tau^2)]^{3/2}}\mathrm{d}\tau\\+\int_{\tau_0}^{\tau_1}\frac{(\Theta_{31}\tau+\Theta_{30})\mathrm{sgn}\langle\tau+1\rangle}{(\lambda_{\mathrm{pn}}+\tau^2)[(l_m^2\lambda_m^+)(\lambda_m+\tau^2)]^{3/2}}\mathrm{d}\tau\end{bmatrix}\tag{C6}$$

where τ_0, τ_1 and λ_{pn}, λ_m are defined in Eqs. (65) and (59) respectively, and

$$\Theta_{11}=\hat{\Gamma}_1(\varpi_1+\varpi_2)+\hat{\Gamma}_0;\quad \Theta_{10}=\hat{\Gamma}_1(\varpi_1-\varpi_2)+\hat{\Gamma}_0$$

$$\Theta_{21}=\Theta_{11};\quad \Theta_{20}=2\Theta_{11}+\Theta_{10}$$

$$\Theta_{31}=2\Theta_{10}+(1-\lambda_{\mathrm{pn}})\Theta_{11};\quad \Theta_{30}=(1-\lambda_{\mathrm{pn}})\Theta_{10}-2\lambda_{\mathrm{pn}}\Theta_{11}$$

$$\Theta_{41}=\Theta_{11};\quad \Theta_{40}=4\Theta_{11}+\Theta_{10}$$

$$\Theta_{51}=2[(3-\lambda_{\mathrm{pn}})\Theta_{11}+2\Theta_{10}];$$
$$\Theta_{50}=2[(3-\lambda_{\mathrm{pn}})\Theta_{10}+2(1-2\lambda_{\mathrm{pn}})\Theta_{11}]$$

$$\Theta_{61}=[(1-\lambda_{\mathrm{pn}})^2-4\lambda_{\mathrm{pn}}]\Theta_{11}+4(1-\lambda_{\mathrm{pn}})\Theta_{10}$$
$$\Theta_{60}=[(1-\lambda_{\mathrm{pn}})^2-4\lambda_{\mathrm{pn}}]\Theta_{10}-4\lambda_{\mathrm{pn}}(1-\lambda_{\mathrm{pn}})\Theta_{11}\tag{C7}$$

As is discussed in Section 6 for Case 3, the integrals involved in Eq. (C6) can be integrated analytically via Eq. (64).

References

Arsenlis, A., Cai, W., Tang, M., et al., 2007. Enabling strain hardening simulations with dislocation dynamics. Model. Simul. Mater. Sci. Eng. 15, 553–595.

Barnett, D.M., 1985. The displacement field of a triangular dislocation loop. Phil. Mag. A 51, 383–387.

Barnett, D.M., 2007. The displacement field of a triangular dislocation loop-a correction with commentary. Phil. Mag. Lett. 87, 943–944.

Brown, L.M., 1967. A proof of Lothe's theorem. Phil. Mag. 15, 363–370.

Burgers, J.M., 1939. Some considerations on the fields of stress connected with dislocations in a regular crystal lattice. Proc. Kon. Ned. Akad. Wetenschap. 42 (293–325), 378–399.

Cai, W., Bulatov, V.V., Pierce, T.G., et al., 2004. Massively-parallel dislocation dynamics simulations. Solid Mechanics and Its Applications, vol. 115. Kluwer Academic Publishers, Dordrecht, pp. 1–11.

Capolungo, L., Beyerlein, I.J., Wang, Z.Q., 2010. The role of elastic anisotropy on plasticity in hcp metals: a three-dimensional dislocation dynamics study. Model. Simul. Mater. Sci. Eng. 18, 1–16.

Chou, Y.T., Yang, H.C., 1973. On Green's tensor funktion for a hexagonal crystal with applications to dislocation theory. Phys. Stat. Sol. (b) 60, 547–556.

Chu, H.J., Pan, E., Wang, J., et al., 2011. Three-dimensional elastic displacements induced by a dislocation of polygonal shape in anisotropic elastic crystals. Int. J. Solids Struct. 48, 1164–1170.

deWit, R., 1960. The continuum theory of stationary dislocations. Solid State Phys. 10, 249–292.

Devincre, B., 1995. Three dimensional stress field expressions for straight dislocation segments. Solid State Commun. 93, 875–878.

Devincre, B., Condat, M., 1992. Model validation of a 3D simulation of dislocation dynamics: discretization and line tension effects. Acta Metall. Mater. 40, 2629–2637.

Devincre, B., Kubin, L.P., 1997. Mesoscopic simulations of dislocations and plasticity. Mater. Sci. Eng. A 234–236, 8–14.

Devincre, B., Kubin, L.P., Lemarchand, C., et al., 2001. Mesoscopic simulations of plastic deformation. Mater. Sci. Eng. A 309–310, 211–219.

Ding, H.J., Chen, W.Q., Zhang, L.C., 2006. Elasticity of Transversely Isotropic Materials. Springer.

Espinosa, H.D., Panico, M., Berbenni, S., et al., 2006. Discrete dislocation dynamics simulations to interpret plasticity size and surface effects in freestanding FCC thin films. Int. J. Plast. 22, 2091–2117.

Fabrikant, V.I., 2004. A new form of the Green function for a transversely isotropic body. Acta Mech. 167, 101–111.

Ghoniem, N.M., Sun, L.Z., 1999. Fast-sum method for the elastic field of three-dimensional dislocation ensembles. Phys. Rev. B 60, 128–140.

Ghoniem, N.M., Tong, S.H., Sun, L.Z., 2000. Parametric dislocation dynamics: A thermodynamics-based approach to investigations of mesoscopic plastic deformation. Phys. Rev. B 61, 913–927.

Gradshteyn, I.S., Ryzhik, I.M., 2007. Table of Integrals, Series, and Products, seventh ed. Elsevier (Singapore) Pte Ltd.

Greer, J.R., Weinberger, C.R., Cai, W., 2008. Comparing the strength of f.c.c. and b.c.c. sub-micrometer pillars: Compression experiments and dislocation dynamics simulations. Mater. Sci. Eng. A 493, 21–25.

Han, X., Ghoniem, N.M., Wang, Z., 2003. Parametric dislocation dynamics of anisotropic crystals. Phil. Mag. 83, 3705–3721.

Hills, D.A., Kelly, P.A., Dai, D.N., et al., 1996. Solution of Crack Problems: The Distributed Dislocation Technique. Kluwer Academic Publishers, Dordrecht.

Hirth, J.P., Lothe, J., 1982. Theory of Dislocations, 2nd ed. John Wiley & Sons, New York.

Indenbom, V.L., Orlov, S.S., 1967. Dislocations in an anisotropic medium. Zh.E.T.F. Pis'ma 6, 826–829.

Indenbom, V.L., Orlov, S.S., 1968. The general solutions for dislocations in an anisotropic medium. In: Proceedings of the Kharkov Conference on Dislocation Dynamics, Acad. Sci. USSR, Moscow, pp. 406–417.

Khraishi, T.A., Hirth, J.P., Zbib, H.M., et al., 2000. The displacement, and strain–stress fields of a general circular Volterra dislocation loop. Int. J. Eng. Sci. 38, 251–266.

Kubin, L.P., Canova, G., Condat, M., et al., 1992. Dislocation microstructures and plastic flow: a 3D simulation. Solid State Phenomena 23–24, 455–472.

Lothe, J., 1967. Dislocation bends in anisotropic media. Phil. Mag. 15, 353–362.

Madec, R., Devincre, B., Kubin, L., et al., 2003. The role of collinear interaction in dislocation-induced hardening. Science 301, 1879–1882.

Madec, R., Devincre, B., Kubin, L.P., 2002. Simulation of dislocation patterns in multislip. Scr. Mater. 47, 689–695.

Mura, T., 1963. Continuous distribution of moving dislocations. Phil. Mag. 8, 843–857.

Ohr, S.M., 1972. Anisotropic elasticity of a prismatic dislocation loop in a hexagonal crystal. J. Appl. Phys. 43, 1361–1365.

Ohr, S.M., 1973. Elastic field of a shear dislocation loop in an anisotropic hexagonal crystal by the Green's function method. Phys. Stat. Sol. (b) 58, 613–621.

Oosterom, A.V., Strackee, J., 1983. The solid angle of a plane triangle. IEEE Trans. Bio. Eng. BME-30, 125–126.

Pan, Y.C., Chou, T.W., 1976. Point force solution for an infinite transversely isotropic solid. ASME. J. Appl. Mech. 43, 608–612.

Paynter, R.J.H., Hills, D.A., Korsunsky, A.M., 2007. The effect of path cut on Somigliana ring dislocation elastic fields. Int. J. Solids Struct. 44, 6653–6677.

Peach, M., Koehler, J.S., 1950. The forces exerted on dislocations and the stress fields produced by them. Phys. Rev. 80, 436–439.

Rhee, M., Zbib, H.M., Hirth, J.P., et al., 1998. Models for long-/short-range interactions and cross slip in 3D dislocation simulation of BCC single crystals. Model. Simul. Mater. Sci. Eng. 6, 467–492.

Rhee, M., Stolken, J.S., Bulatov, V.V., et al., 2001. Dislocation stress fields for dynamic codes using anisotropic elasticity: methodology and analysis. Mater. Sci. Eng. A 309–310, 288–293.

Schwarz, K.W., 1999. Simulation of dislocations on the mesoscopic scale. I. Methods and examples. J. Appl. Phys. 85, 108–119.

Senger, J., Weygand, D., Gumbsch, P., et al., 2008. Discrete dislocation simulations of the plasticity of micro-pillars under uniaxial loading. Scripta Mater. 58, 587–590.

Tupholme, G.E., 1974. Dislocation loops in hexagonal crystals. J. Mech. Phys. Solids 22, 309–321.

Verdier, M., Fivel, M., Groma, I., 1998. Mesoscopic scale simulation of dislocation dynamics in fcc metals: principles and applications. Model. Simul. Mater. Sci. Eng. 6, 755–770.

von Blanckenhagen, B., Arzt, E., Gumbsch, P., 2004. Discrete dislocation simulation of plastic deformation in metal thin films. Acta Mater. 52, 773–784.

Wang, C.Y., 1996. The stress field of a dislocation loop in an anisotropic solid. J. Mech. Phys. Solids 44, 293–305.

Wang, Z.Q., Beyerlein, I.J., LeSar, R., 2009. Plastic anisotropy in fcc single crystals in high rate deformation. Int. J. Plast. 25, 26–48.

Wang, Z.Q., Ghoniem, N., Swaminarayan, S., et al., 2006. A parallel algorithm for 3D dislocation dynamics. J. Comput. Phys. 219, 608–621.

Weygand, D., Poignant, M., Gumbsch, P., et al., 2008. Three-dimensional dislocation dynamics simulation of the influence sample size on the stress–strain behavior of fcc single-crystalline pillars. Mater. Sci. Eng. A 483–484, 188–190.

Willis, J.R., 1970. Stress fields produced by dislocations in anisotropic media. Phil. Mag. 21, 931–949.

Yin, J., Barnett, D.M., Cai, W., 2010. Efficient computation of forces on dislocation segments in anisotropic elasticity. Model. Simul. Mater. Sci. Eng. 18, 045013.

Yu, H.Y., Sanday, S.C., 1994. Dislocations and disclinations in transversely isotropic elastic solids. Phil. Mag. A 70, 725–738.

Zbib, H.M., de la Rubia, T.D., Rhee, M., et al., 2000. 3D dislocation dynamics: stress–strain behavior and hardening mechanisms in fcc and bcc metals. J. Nucl. Mater. 276, 154–165.

Zbib, H.M., Rhee, M., Hirth, J.P., 1998. On plastic deformation and the dynamics of 3D dislocations. Int. J. Mech. Sci. 40, 113–127.

Zhou, C.Z., LeSar, R., 2012. Dislocation dynamics simulations of plasticity in polycrystalline thin films. Int. J. Plast. 30–31, 185–201.